TÜBİTAK

Turkish Journal of Biology

http://journals.tubitak.gov.tr/biology/

Research Article

Turk J Biol
(2016) 40: 684-693
© TÜBİTAK
doi:10.3906/biy-1505-6

The global transcriptional response of a raw starch-degrading amylolytic *Saccharomyces cerevisiae* strain to oxygen limitation and genetic modification

Ceyda KASAVI[1,*], Serpil ERASLAN[1], Ebru TOKSOY ÖNER[2], Betul KIRDAR[1]
[1]Department of Chemical Engineering, Boğaziçi University, İstanbul, Turkey
[2]Department of Bioengineering, Marmara University, İstanbul, Turkey

Received: 04.05.2015 • **Accepted/Published Online:** 13.09.2015 • **Final Version:** 18.05.2016

Abstract: This study investigates the global transcriptional response of *Saccharomyces cerevisiae* strain WTPB-G, which was developed by transforming laboratory strain FY23 with the pPB-G plasmid expressing the *Bacillus subtilis* α-amylase and the *Aspergillus awamori* glucoamylase as a fusion protein. Genome-wide analysis of transcript levels revealed the cellular mechanisms and the related pathways that were affected by the genetic modification, which conferred the ability of starch utilization to wild-type cells by the introduction of a plasmid-harboring gene encoding the amylolytic activity. Fermentations were carried out in media containing glucose as the only carbon source under aerated and microaerated conditions, and the effect of aeration was also investigated in terms of fermentation properties and transcriptional response. The genome-wide gene expression analysis highlighted that plasmid replication induced cell wall organization and biogenesis, and repressed approximately 20% of the genes involved in ribosome biogenesis and RNA processing. Although oxygen limitation was found to be less effective in the transcriptional changes, a link between oxygen limitation and genes involved in oxidation-reduction, pH reduction, phosphate-containing compounds, and lipid and fatty acid processes was observed.

Key words: Amylolytic yeast, *Saccharomyces cerevisiae*, transcriptome, bioethanol

1. Introduction

Depletion of fossil fuels and environmental problems make biomass an attractive source of renewable energy (Yamada et al., 2011). One-step conversion of biomass to ethanol is considered the most cost-effective route to renewable fuels (Elkins et al., 2010). Besides the fermentation substrate, the selection of an appropriate production organism is also important for the economic viability of fuel ethanol. *Saccharomyces cerevisiae* is a major microbial species that has been exploited for ethanol production due to its high fermentation rate and ethanol tolerance (Choi et al., 2009; Inderwildi and King, 2009; Kim et al., 2010). After cellulose, starch is the second most abundant plant polysaccharide and hence an important renewable resource for bioethanol production.

Starch is a biopolymer and is defined as a homopolymer consisting of only one monomer, D-glucose. These D-glucose structures are linked together via α-1,4 and α-1,6 glycosidic linkages. The α-1,4 linkages produce linear chains that primarily comprise molecules called amylose, whereas the α-1,6 linkages serve as branching points to produce branched chain molecules called amylopectin. Amylose forms a minor part (20%–30%) of starch and amylopectin forms the major part (70%–80%) (Yamada et al., 2009). In order to produce ethanol from starch, it is necessary to break down the chains of this carbohydrate into six carbon sugars, which can be converted into ethanol by yeasts (Gray et al., 2006; Bai et al., 2008; Balat et al., 2008). The degradation of raw starch into glucose is a multistep enzymatic process, which involves its gelatinization by cooking and liquefaction by α-amylase, followed by saccharification to glucose by glucoamylase (Wong et al., 2007; Favaro et al., 2010). The starch-based bioethanol industry has been commercially viable for about 30 years and corn and wheat are the most utilized sources of starch employed for ethanol production (Gray et al., 2006; Balat et al., 2008; Goyal et al., 2008).

Hydrolyzation of starch is catalyzed by α-amylase and glucoamylase. At the first step, a thermostable α-amylase enzyme is used to produce soluble dextrins by hydrolyzing α-1,4 bonds. In the saccharification step, glucoamylase is used to convert the liquefied starch into C6 sugars (Bothast and Schlicher, 2005; Sánchez and Cardona, 2008), and then, in the fermentation step, C6 sugars are converted

* Correspondence: ceydakasavi@gmail.com

into ethanol (Toksoy Öner et al., 2005). When starch is used as a raw material, the amylases are strongly inhibited by hydrolysis products such as glucose. This problem can be overcome by a simultaneous saccharification and fermentation process, which combines enzymatic hydrolysis with fermentation (Sánchez and Cardona, 2008; Shen et al., 2008).

S. cerevisiae can ferment certain mono- and disaccharides, such as glucose, fructose, maltose, and sucrose, but it lacks the ability to utilize starch and hence to synthesize and secrete necessary amylolytic enzymes that are required for the bioconversion of starch to ethanol. Therefore, consolidated bioprocessing of starchy materials to bioethanol by *S. cerevisiae* has required significant strain improvement efforts to introduce this ability to *S. cerevisiae* strains (Favaro et al., 2010). A plasmid-based system, WTPB-G (Toksoy Öner et al., 2005), was developed by transforming standard laboratory strain FY23 with the pPB-G plasmid (de Moraes et al., 1995) that contains the *Bacillus subtilis* α-amylase and the *Aspergillus awamori* glucoamylase coding sequences, expressed under the control of the constitutive PGK1 promoter as an excreted bifunctional fusion protein (Toksoy Öner et al., 2005). Although significant improvements were thereby achieved with the amylolytic *S. cerevisiae* strain WTPB-G in ethanol yield from soluble starch by optimizing fermentation conditions, a time-dependent loss of amylolytic activity was observed (Toksoy Öner, 2006).

The aim of this study is to investigate the effect caused in a wild-type strain by the presence of an extrachromosomal self-replicating element in the form of a recombinant multicopy plasmid, which conferred the ability of starch utilization to wild-type cells. For this purpose, the fermentation performances of wild-type FY23 and the plasmid-bearing strain WTPB-G were comparatively examined in batch cultures, in which the cultivation temperature and pH were controlled under aerated and microaerated conditions. Fermentations were carried out in media containing glucose as the sole carbon source. The investigation of the genome-wide gene expression profiles revealed that the presence of a plasmid encoding a fusion protein caused changes in the expression levels of genes. These changes were associated with cell wall biogenesis, ribosome biogenesis, and RNA processing, whereas oxygen limitation resulted in the significant expression of genes involved in protein modification, respiration, and energy mechanisms.

2. Materials and methods

2.1. Strains and growth media

The *S. cerevisiae* WTPB-G strain (Toksoy Öner et al., 2005), generated by transforming the parental haploid FY23 strain with the pPB-G plasmid (de Moraes et al., 1995) that contains *B. subtilis* α-amylase and *A. awamori* glucoamylase genes expressed under the control of the constitutive PGK1 promoter as an excreted bifunctional fusion protein, was used in this study.

S. cerevisiae strains were kept in glycerol stock solutions at –80 °C. Frozen glycerol cultures were used by streaking on selective yeast minimal media (YMM; 20 g L^{-1} D-glucose, 6.7 g L^{-1} yeast nitrogen base without amino acids, 0.1 g L^{-1} tryptophan, 0.1 g L^{-1} uracil) agar plates for the preparation of master plates. Single colonies formed at 30 °C were transferred to YPDS (4 g L^{-1} D-glucose, 20 g L^{-1} peptone, 10 g L^{-1} yeast extract, 10 g L^{-1} soluble starch) and YMM plates and incubated at 30 °C to select for amylolytic activity. YPDS plates were stained with iodine vapor until the formation of large visible zones around the colonies, indicating the utilization of starch. Colonies with larger haloes were picked from replica YMM plates and used for inoculum preparation. Agar plates were prepared by adding 18 g L^{-1} agar to the media.

Precultures were inoculated with a single colony of cells taken from YMM agar plates and incubated in YMM medium at 30 °C and 180 rpm.

2.2. Cultivation conditions and sampling

For batch bioreactor cultivations, cells were cultivated in fully controlled 2-L B-Braun BIOSTAT B Plus fermenters with a working volume of 1.5 L in YMM medium containing glucose as the sole carbon source. The temperature was kept constant at 30 °C, and agitation was set to 400 rpm at all times throughout the fermentation. pH was kept constant at 5.6 by controlling with 0.5 M NaOH and HCl. The dissolved oxygen (DO) saturation was preserved above 90% throughout the experiment via a constant flow of air at 0.75 L/min in aeration-controlled cultivations. To provide microaerated conditions, cultivations were initially brought to a DO saturation of 100% and air supply was turned off throughout the fermentation. Optical densities (ODs) were monitored by spectrophotometric measurements at 600 nm wavelength until a steady state was reached. All experiments were carried out in duplicate.

Sampling was carried out during the exponential phase of growth for the determination of μ_{max}, extracellular glucose, and ethanol concentrations. Confidence intervals of 95% were provided for μ_{max}. Extracellular metabolite concentrations were determined by using enzymatic analysis kits (Sigma) as described by the manufacturer. Samples from the steady-state culture were used to gravimetrically determine the dry cell weight (DCW) of cultures. Cells were first recovered from 1 mL of culture samples through centrifugation, then washed with distilled water three times and dried at 70 °C until constant weight was achieved. Reported DCW values are the average of five biological and two technical replicates for each data point. For the transcriptome analysis, samples were taken

at the midexponential phase of growth (OD_{600} ≈ 0.7–0.9), immediately frozen in liquid nitrogen, and stored at –80 °C until RNA isolation.

2.3. Determination of amylase activity

Protein purification was performed with culture supernatants diluted with two volumes of ice-cold acetone and centrifuged at 10,000 rpm for 20 min at 4 °C to recover extracellular precipitates (Birol et al., 1998). To assay for α-amylase activity, pellets were dissolved in 50 mM NaAc buffer (pH 5.9), and 0.5 g of soluble starch was added to 100 mL of boiling 50 mM NaAc buffer (pH 5.9). Appropriately diluted enzyme solutions of 100 µL were incubated with 500 µL of starch solution at 40 °C for 10 min and then 200 µL of this reaction mix was mixed with 5 mL of iodine solution (10 mM KI and 2 mM I_2). Degradation of starch was measured at 620 nm against 200 µL of water in 5 mL of iodine solution as a blank. One unit of α-amylase activity was defined as the quantity of enzyme required to hydrolyze 0.1 mg of starch in 10 min at 40 °C.

For the glucoamylase activity assay, pellets were dissolved in 50 mM NaAc buffer (pH 4.5) and 0.5 g of soluble starch was added to 100 mL of boiling 50 mM NaAc buffer (pH 4.5). Afterwards, 50 µL of enzyme solution was mixed with 500 µL of starch solution and incubated at 40 °C for 10 min. An aliquot (200 µL) of this reaction mix was used to assay for glucose. Glucose concentration was determined using enzymatic analysis kits. One unit of glucoamylase activity was defined as the amount of enzyme that released 1 mM of glucose per minute from starch.

2.4. RNA isolation and microarray analysis

RNA isolation was carried out in a robotic workstation, QIAcube (QIAGEN, USA), using the enzymatic lysis protocol as described by the QIAGEN RNeasy Mini Kit (Cat. No. 74106). The quality and quantity of the isolated RNA were checked via spectrophotometric analysis using a UV-Vis spectrophotometer (NanoDrop ND-1000, Thermo Fisher Scientific Inc., USA). RNA samples were subjected to a second quality check step before being used in microarray analysis. RNA integrity number (RIN) values were checked using a microfluidics-based platform (Bioanalyzer 2100, Agilent Technologies, USA) with an RNA 6000 Nano Kit (Agilent Technologies, USA) and samples with RIN values of 7–10 were processed.

First-strand cDNA was synthesized and then converted into double-stranded DNA initially from 100 ng of total RNA using the GeneChip 3' IVT Express Kit (Affymetrix Inc., USA). This double-stranded cDNA was used as a template for in vitro transcription and synthesis of biotin-labeled aRNA. The final product was purified and quantified using the NanoDrop spectrophotometer before fragmentation. The purification and fragmentation steps were carried out using GeneChip reagents. Fragmented aRNA was evaluated using the Agilent 2100 Bioanalyzer (Agilent Technologies, Germany). Affymetrix Yeast 2.0 arrays were prepared for hybridization using the reagents supplied in the GeneChip Hybridization, Wash, and Stain Kit. A total of 5 µg of aRNA was loaded onto 169 format arrays and hybridized for 16 h. The chips were then loaded into a fluidics station for washing and staining using the Affymetrix Command Console 3.0.1 Fluidics Control Module with Mini Euk 2v3 protocol. Finally, the chips were loaded onto the Affymetrix GeneChip Scanner 3000. All applications were performed as described in the Affymetrix GeneChip Expression Analysis Technical Manual. The microarray data from this study were submitted to ArrayExpress at the European Bioinformatics Institute under accession number [E-MTAB-3545], in compliance with MIAME guidelines.

2.5. Microarray data acquisition and analysis

For the analysis of transcriptomics data, cell files were normalized via quantile normalization using RMA (Bolstad et al., 2003) as implemented in the affy package (Gautier et al., 2004) of the R/Bioconductor suite of tools (Gentleman et al., 2004).

The hierarchical clustering of the conditions was carried out via the Multi Experiment Viewer (MeV) (Saeed et al., 2006), with the distance and the linkage metric selected as the Pearson correlation and the average linkage, respectively.

Significantly expressed genes were identified from normalized log-expression values using two-way analysis of variance (ANOVA) implemented in MeV, and a 0.001 P-value threshold was maintained. The two-way ANOVA revealed the genes that were significantly expressed in response to the presence of the recombinant vector and the constitutive expression of the amylolytic genes on that plasmid and the aeration. The genes that were affected by the interactive effect of the plasmid presence and aeration were identified as the genes responsive to the changes in both factors at the same time. These statistically significant genes were used as inputs for gene set enrichment analysis based on Gene Ontology (GO) annotations. All GO analyses were performed via the Generic GO Term Finder (Boyle et al., 2004) using a *Saccharomyces* Genome Database filter, with a P-value cut-off of 0.01.

2.6. Reporter features analysis

The regulatory pathways that were affected by the presence of plasmid and oxygen limitation were identified by Reporter Features analysis (Patil and Nielsen, 2005; Oliveira et al., 2008), implemented in the BioMet Toolbox (Cvijovic et al., 2010). The Reporter Feature algorithm was used for the integration of regulome with transcriptome. Transcription factors (TFs) in the consensus list described in the Yeastract database (Teixeira et al., 2013) were considered for the construction of a regulatory network

in yeast. The yeast regulatory network was constructed by extracting tabthe TF–protein interactions with direct evidence in the Yeastract database (Cankorur-Cetinkaya et al., 2013; Kasavi et al., 2014). A P-value threshold of 0.01 was maintained to determine the Reporter TFs.

3. Results

3.1. Growth characteristics of batch fermentations

The growth characteristics of the batch cultures were investigated during the exponential and stationary phases of growth. The fermentation performances of the plasmid-bearing strain WTPB-G, together with the wild-type strain FY23, grown on YMM, were investigated and compared under both microaerated and aerated conditions (Figure 1). Maximum biomass, ethanol, and glycerol concentrations reached by the cultures, as well as their glucose utilization rates and maximum specific growth rates, were measured (Table 1).

Under aerated conditions, both strains reached higher biomass concentrations. Aeration had a more profound effect on the growth properties of the WTPB-G strain than the wild-type strain. Oxygen limitation caused a 21% and 34% decrease in biomass concentrations of FY23 and WTPB-G cultures, respectively. A similar effect was also observed in the μ_{max} values of both cultures. Furthermore, oxygen limitation caused an approximately 3-fold increase in the glycerol concentrations and yields of both strains.

At the end of each fermentation, carried out under aerated and microaerated conditions with the WTPB-G strain, enzymes in the cell-free media were precipitated with acetone and crude enzyme solutions were subjected to amylase activity assays. The α-amylase activities were 20 U/mL culture (9434 U/g DCW) and 22 U/mL culture (8178 U/g DCW), and glucoamylase activities were 227 U/L culture (107 U/g DCW) and 278 U/L culture (103 U/g DCW) under microaerated and aerated conditions, respectively.

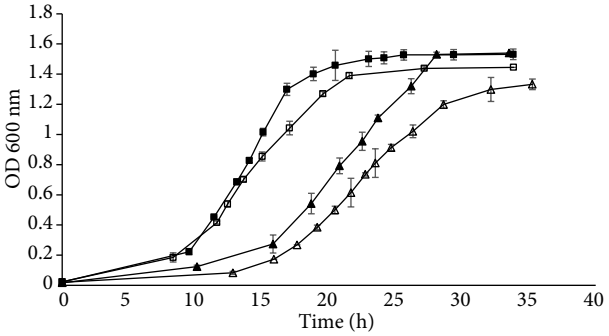

Figure 1. Growth profiles of FY23 (□, ■) and WTPB-G (▲, △) strains under aerated (filled symbols) and microaerated (open symbols) conditions.

3.2. Global transcriptional response of S. *cerevisiae* strains

In order to provide further insight into the molecular mechanisms affected by the presence of plasmid and the secretion of fusion proteins, the genome-wide transcriptional responses of the recombinant amylolytic *S. cerevisiae* strain WTPB-G and the reference strain were comparatively investigated. Since higher ethanol concentrations were reached by WTPB-G and its parent strain FY23 cultures under aerated conditions when compared to microaerated conditions, the mechanisms affected by aeration were also investigated. The two parameters of interest were strain at two levels, reference strains FY23 and WTPB-G, and aeration at two levels, aerated and microaerated conditions. A 2 × 2 factorial design enabled the investigation of the effect of these factors

Table 1. Fermentation parameters of *S. cerevisiae* strains grown in media containing glucose as the sole carbon source.

Parameter	Aerated		Microaerated	
Strains	FY23	WTPB-G	FY23	WTPB-G
Biomass (g L^{-1})	2.59 ± 0.13	2.69 ± 0.11	2.26 ± 0.12	2.12 ± 0.09
μ_{max} (h^{-1})	0.270 ± 0.011	0.214 ± 0.001	0.236 ± 0.004	0.203 ± 0.009
Max. ethanol conc. (g L^{-1})	4.93 ± 0.25	4.79 ± 0.22	4.26 ± 0.31	3.91 ± 0.15
Glucose utilized (g L^{-1})	17.61 ± 0.54	17.58 ± 0.62	18.52 ± 0.71	18.14 ± 0.45
Y_{ps} (g ethanol g^{-1} glucose)	0.28	0.27	0.23	0.22
Y_{px} (g ethanol g^{-1} biomass)	1.90	1.78	1.89	1.85
Max. glycerol conc. (g L^{-1})	0.085 ± 0.012	0.092 ± 0.021	0.152 ± 0.009	0.174 ± 0.018
$Y_{gly/s}$ (g glycerol g^{-1} glucose)	0.003	0.003	0.008	0.010

on the transcriptional response of yeast cells. The samples collected at the midexponential phase of growth were used for transcriptomic analysis. The genes showing significant changes in their expression levels were identified from the normalized log-expression values via two-way ANOVA. Two-way ANOVA assessed the transcriptional changes according to three factors: effect of the recombinant vector and the constitutive expression of the amylolytic genes on that plasmid, effect of aeration, and interaction effect of these two factors.

The hierarchical clustering of conditions, using normalized microarray data, revealed strains as the key determinant for the arrangement of different clusters. The analysis resulted in the clustering of the conditions into two major clusters (Figure 2). The transcript profiles of wild-type cultures were clustered together under microaerated and aerated conditions, whereas the transcript profiles of WTPB-G cultures under microaerated and aerated conditions formed a different cluster. Moreover, the replicate fermentations were clustered together for each strain under similar conditions.

3.3. Identification of significantly expressed genes

The genes showing significant changes ($P < 0.001$) in their expression levels were identified via two-way ANOVA. When WTPB-G was compared to the reference strain, a total of 950 (524 up, 426 down) genes displayed significantly altered expression levels in response to the presence of a plasmid synthesizing a bifunctional protein, which may catalyze the one-step conversion of starch to ethanol (Table S1). Genes whose expression levels were significantly up- and downregulated under oxygen limitation were screened using microarray data obtained from samples collected at the midexponential phase of growth and 579 (309 up, 271 down) genes showed a statistically significant difference in their expression levels when the microaerated condition was compared to the aerated condition (Table S2). Moreover, 72 genes were significantly expressed in response to the interactive effect of the presence of a plasmid synthesizing a bifunctional protein, which may catalyze the one-step conversion of starch to ethanol, and oxygen limitation (Table S3).

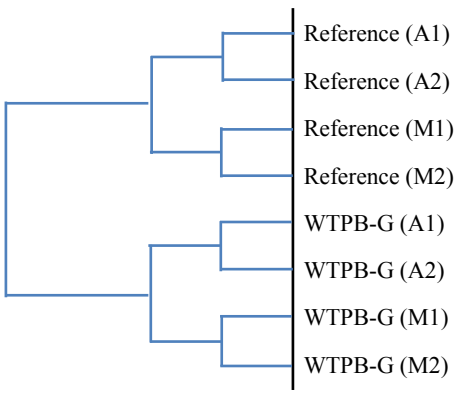

Figure 2. Hierarchical clustering of experimental conditions using normalized microarray data (M and A represent the microaerated and aerated conditions, respectively).

Genes whose expression levels were significantly changed in response to the presence of the recombinant vector and the constitutive expression of the amylolytic genes on that plasmid were defined as strain-significant genes, and genes whose expression levels were significantly changed in response to oxygen limitation were defined as aeration-significant genes. Significantly enriched categories of the up- and downregulated strain-significant and aeration-significant genes were analyzed using Amigo.

3.4. Transcriptional response to the presence of the recombinant vector and the constitutive expression of the amylolytic genes on the plasmid

In response to the presence of a plasmid synthesizing a bifunctional protein, which may catalyze the one-step conversion of starch to ethanol, the upregulated genes were significantly enriched for cell wall organization and biogenesis (Table S4) and the downregulated genes were significantly enriched for growth-associated processes including ribosome biogenesis and RNA processing (Table S5).

The manual investigation of genes related to DNA replication revealed that 5 genes (*POL1*, *POL2*, *RFA1*, *CDC9*, and *RNH201*), encoding proteins related to DNA replication in *S. cerevisiae*, were downregulated in response to the presence of the recombinant vector and the constitutive expression of the amylolytic genes on that plasmid. *POL1* is an essential gene that encodes the largest subunit of the DNA polymerase (I) alpha and is required for the initiation of DNA replication. *POL2* is also an essential gene, encoding a catalytic subunit of DNA polymerase (II) epsilon, which is a chromosomal DNA replication polymerase that exhibits proofreading exonuclease activity. *POL2* is also involved in DNA synthesis during DNA repair. *RFA1* encodes a subunit of heterotrimeric replication protein A (RPA), which is a highly conserved, single-stranded DNA-binding protein. *RFA1* plays a key role in DNA metabolic pathways such as DNA replication, repair, and recombination. *CDC9*, an essential gene, encodes a DNA ligase found in the nucleus and mitochondria. Cdc9p is an essential enzyme that joins Okazaki fragments during DNA replication, and it also acts in nucleotide excision repair, base excision repair, and recombination. *RNH201* encodes a ribonuclease H2 catalytic subunit that removes RNA primers during Okazaki fragment synthesis. Furthermore, the presence of the plasmid resulted in the upregulation of 42 genes encoding proteins whose abundance increases in response to DNA replication stress.

3.5. Transcriptional response to aeration

Clustering of conditions indicated that aeration caused a less effective change than plasmid harboring on the transcriptional response. The significantly enriched biological processes of aeration-significant genes are provided in Tables S6 and S7.

In response to oxygen limitation, upregulated genes were found to be enriched with various catabolic processes and cellular response to stimulus. The downregulated aeration-significant genes were found to be significantly enriched with nitrogen and organonitrogen compound metabolic and biosynthetic processes, as well as organophosphate and lipid biosynthetic processes. Further investigation of the downregulated genes indicated that a total of 29 genes involved in oxidation-reduction processes, 5 genes involved in pH reduction, 11 genes involved in the cofactor metabolic process, and 8 genes involved in the coenzyme biosynthetic process were downregulated in response to oxygen limitation. Furthermore, oxygen limitation resulted in the downregulation of genes involved in lipid and fatty acid, carbohydrate, and phosphate-containing compound metabolic processes.

3.6. Transcriptional response to the interactive effect of factors

A total of 72 genes were significantly expressed in response to the interactive effect of the presence of a plasmid, synthesizing a bifunctional protein and oxygen limitation and described as an interaction-significant gene. When the aerated condition was compared to the microaerated condition, 32 genes were upregulated and 40 genes were downregulated in the reference strain. Under similar conditions, 25 genes were upregulated and 47 genes were downregulated in WTPB-G. When the significantly expressed genes in WTPB-G in comparison to the reference strain were investigated, 32 genes were upregulated and 40 genes were downregulated under aerated conditions, and 37 genes were upregulated and 35 were downregulated under microaerated conditions. The number of interaction-significant genes under each condition is presented in Figure 3.

The significantly expressed genes in response to the interactive effect were not found to be significantly enriched with any particular GO biological process term for each group. A total of 14 genes had unknown GO biological process terms. The up- and downregulated genes were analyzed using the Generic GO Term Finder (Boyle et al., 2004) to shed light on the biological processes that these genes were annotated to (Tables S8 and S9). Although all biological processes were included in the supplementary tables, terms that at least four genes annotated to were taken into consideration.

The assessment of the aerated conditions in conjunction with the microaerated conditions revealed the upregulation of genes involved in protein complex biogenesis, Golgi vesicle transport, and lipid metabolic process and the downregulation of genes involved in mitochondrion organization, nucleobase-containing small molecule metabolic process, carbohydrate metabolic process, transmembrane transport, and protein complex biogenesis in WTPB-G strain. The same comparison pointed to the induction of genes associated with mitochondrion organization, lipid metabolic process, and protein complex biogenesis and to the repression of genes associated with transmembrane transport, regulation of organelle organization, and protein complex biogenesis in the reference strain.

The comparison of WTPB-G and the reference strain indicated the presence of genes associated with protein complex biogenesis, Golgi vesicle transport, and a nucleobase-containing small molecule metabolic

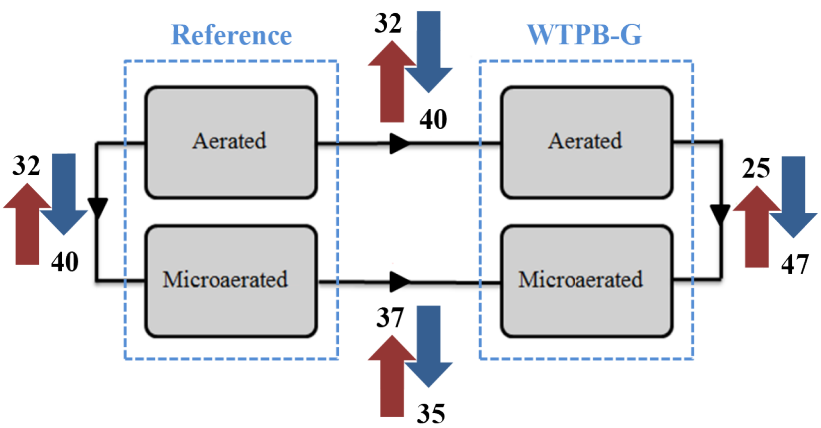

Figure 3. Number of genes that were significantly and differentially expressed in response to the interactive effect of plasmid bearing and oxygen limitation in FY23 (as a reference) and WTPB-G strains.

process among the upregulated genes under aerated conditions. Genes related to mitochondrion organization, monocarboxylic acid metabolic process, lipid metabolic process, carbohydrate metabolic process, and transmembrane transport were found to be downregulated under similar conditions. Under microaerated conditions, genes that play a role in protein-complex biogenesis, lipid metabolic process, ion transport, Golgi vesicle transport, mitochondrion organization, nucleobase-containing small molecule metabolic process, and transmembrane transport were upregulated; genes related to carbohydrate metabolic process were downregulated.

3.7. Analysis of regulation of transcriptional response to the presence of a plasmid synthesizing a bifunctional protein and oxygen limitation in genetically engineered *S. cerevisiae* cells

The transcriptional response of the *S. cerevisiae* strain to the presence of pPB-G plasmid and oxygen limitation was analyzed in the context of regulatory networks using Reporter TF Analysis to shed light on the affected regulatory machineries.

Reporter TF analysis identified 3 TFs (Rts2p, Hac1p, and Fkh1p) around which genes were affected in response to the presence of the recombinant vector and the constitutive expression of the amylolytic genes on that plasmid. Rts2p is a basic zinc-finger protein, similar to human and mouse Kin17 proteins, which are chromatin-associated proteins involved in UV response and DNA replication. Hac1p is a basic leucine zipper TF, which regulates the unfolded protein response. The protein abundance of Hac1p increases in response to DNA replication stress. Fkh1p plays a minor role in the expression of G2/M phase genes, negatively regulates transcriptional elongation, and has a positive role in chromatin silencing.

Reporter TF analysis identified 2 TFs (Mot3p and Rox1p) around which genes were affected in response to oxygen limitation. Mot3p is a transcriptional repressor involved in the repression of a subset of hypoxic genes by Rox1p. Rox1p is a repressor of hypoxic genes and mediates the aerobic transcriptional repression of hypoxia-induced genes such as *COX5* and *CYC7*.

4. Discussion

The assessment of the fermentation performance of FY23 and WTPB-G cultures under aerated and microaerated conditions revealed that oxygen limitation led to decreased biomass concentrations and μ_{max} values for both cultures. *S. cerevisiae* physiology was affected by aeration, which is a significant control factor during alcoholic fermentation. It has been reported that aeration improved the fermentation performance of *S. cerevisiae* (Alfenore et al., 2004; Guimarães et al., 2008; Sanchez-Gonzalez et al., 2009). Additionally, in this study, higher ethanol concentrations were obtained under aerated conditions with both strains. Furthermore, oxygen limitation resulted in an increase in glycerol concentrations and yields of both strains. This finding was consistent with the formation of glycerol at a much higher yield under anaerobic conditions than under aerobic conditions. Under oxygen-limited conditions, glycerol is formed to modulate NADH and NADPH levels to restore the redox balance in the cell (Costenoble et al., 2000; Alfenore et al., 2004). Under both aerated and microaerated conditions, the WTPB-G strain had a lower specific growth rate than FY23 (0.214 h^{-1} versus 0.270 h^{-1} under aerated conditions and 0.203 h^{-1} versus 0.236 h^{-1} under microaerated conditions). The maintenance of a plasmid and its expression in a yeast cell impose a metabolic burden and affect the cell's ability to grow (Ow et al., 2006; Karim et al., 2013). Therefore, the presence of the plasmid and the expression of α-amylase and glucoamylase as a fusion protein resulted in reduced growth rate of the WTPB-G strain. At the end of each fermentation carried out under aerated and microaerated conditions with the WTPB-G strain, the amylase activities were also determined. Since fermentations were carried out in media containing only glucose as a carbon source, the α-amylase activities of WTPB-G under both conditions were found to be very low when compared to earlier reports where complex media were used for fermentations. Glucoamylase and α-amylase activities were reported to be within the ranges of 300–9000 U/mL and 700–1200 U/mL, respectively, in media containing 5% starch (Toksoy Öner et al., 2005).

The global transcriptional responses of the recombinant amylolytic *S. cerevisiae* strain WTPB-G and the reference strain were comparatively investigated to identify the molecular mechanisms affected by the presence of the plasmid and the secretion of fusion proteins, as well as oxygen limitation. Two-way ANOVA enabled the assessment of the effect of the presence of the recombinant vector and the constitutive expression of the amylolytic genes on that plasmid, the effect of aeration, and the interaction effect of these two parameters. The hierarchical clustering of conditions based on the expression values showed that the microaerated and aerated conditions were clustered together for both strains. Therefore, the effect of aeration was found to be less determinative on the transcriptional response than the effect of harboring a genetically engineered plasmid, which produces a bifunctional enzyme to catalyze the one-step conversion of starch to ethanol.

In response to the presence of the plasmid and the expression of the amylolytic genes on that plasmid, ribosome biogenesis was found to be repressed. Ribosome biogenesis is an essential cellular process and the inhibition of this process may result in terminated

cell growth, even under optimal growth conditions (Li et al., 2009). The downregulation of genes associated with ribosome biogenesis supported the reduced growth rate of the WTPB-G strain. There are 444 known genes involved in ribosome biogenesis in *S. cerevisiae*, and only 88 were downregulated in the WTPB-G strain. Therefore, the remaining genes enable this yeast to grow under controlled conditions and to produce ethanol. Moreover, protein synthesis is an energy-cost activity in the cell. The downregulation of the genes related to ribosome biogenesis and RNA processing might result in reduced protein synthesis, which is not essential for the cell to grow and help to save energy. Moreover, a total of 5 gene-encoding proteins related to DNA replication in *S. cerevisiae* were repressed, whereas 42 gene-encoding proteins, whose abundance increases in response to DNA replication stress, were induced in response to the presence of the plasmid and the expression of the amylolytic genes on that plasmid. The maintenance of a plasmid and its expression in a yeast cell imposes a metabolic burden and affects the cell's ability to grow (Ow et al., 2006; Karim et al., 2013), which was found to be in accordance with the repression of growth-associated processes in response to the presence of the plasmid and the expression of the amylolytic genes on that plasmid. Since plasmid DNA replicates as chromosomal DNA, plasmid-associated metabolic burden might be the reason for increased DNA replication stress in the WTPB-G strain. Moreover, the inhibitory effect of plasmid burden on growth might result in the repression of DNA synthesis. However, the activation of genes associated with DNA replication stress would preserve genome integrity during DNA replication.

In response to oxygen limitation, genes involved in oxidation-reduction and pH reduction processes, cofactor metabolic process, coenzyme biosynthetic process, lipid and fatty acid metabolic processes, and phosphate-containing compound metabolic process were found to be downregulated. *S. cerevisiae* requires a maintained cellular redox balance in order to sustain metabolism and growth. Redox cofactors participate in biochemical reactions involving oxidation-reduction (Heux et al., 2006). The downregulation of genes related to oxidation-reduction in response to oxygen limitation is consistent with the decreased growth of both the WTPB-G and reference strain cultures under microaerated conditions. Moreover, the downregulation of oxidation-reduction and coenzyme processes possibly decreases the amount of generated energy in the cells. This might result in the repression of energy-requiring metabolic processes such as the phosphate-containing compound metabolic process and lipid and fatty acid metabolic processes.

The integrative analysis of the regulome and transcriptome revealed the TFs around which genes were affected by the presence of the pPB-G plasmid and the expression of the amylolytic genes on that plasmid and oxygen limitation. Reporter TFs around which genes were affected in response to the presence of the plasmid were found to be associated with DNA replication, which was reported to be important for plasmid stability. Therefore, the existence of TFs involved in DNA replication is consistent with the presence of the self-replicating plasmid. TFs associated with the regulation of hypoxic gene expression were identified as Reporter TFs in response to oxygen limitation. The identification of TFs that regulate the expression of hypoxic genes is in good agreement with the effect of oxygen limitation during fermentation.

In conclusion, investigating the changes of the plasmid-bearing *S. cerevisiae* strain WTPB-G at the transcriptional level provided information on the molecular mechanisms underlying the presence of a plasmid synthesizing a bifunctional protein, which may catalyze the one-step conversion of starch to ethanol. In future studies, the high-level expression of amylolytic enzymes by multicopy integration of their coding sequences into the genome of a wild-type strain should result in stable extracellular amylolytic activities against raw starch substrates, such as agricultural and agroindustrial residues, and enable their conversion into fermentable sugars for ethanol production.

Acknowledgments

The authors gratefully acknowledge the Turkish State Planning Organization (DPT09K120520), the Boğaziçi University Research Fund (Project No. 6530), and TÜBİTAK (Project No. 110M692) for their financial support of this research.

References

Alfenore S, Cameleyre X, Benbadis L, Bideaux C, Uribelarrea JL, Goma G, Molina-Jouve C, Guillouet SE (2004). Aeration strategy: a need for very high ethanol performance in *Saccharomyces cerevisiae* fed-batch process. Appl Microbiol Biotechnol 63: 537-542.

Bai FW, Anderson WA, Moo-Young M (2008). Ethanol fermentation technologies from sugar and starch feedstocks. Biotechnol Adv 26: 89-105.

Balat M, Balat H, Öz C (2008). Progress in bioethanol processing. Prog Energy Combust Sci 34: 551-573.

Birol G, Önsan Zİ, Kırdar B, Oliver SG (1998). Ethanol production and fermentation characteristics of Recombinant *Saccharomyces cerevisiae* strains grown on starch. Enzyme Microb Technol 22: 672-677.

Bolstad BM, Irizarry R, Astrand M, Speed TP (2003). A comparison of normalization methods for high density oligonucleotide array data based on variance and bias. Bioinformatics 19: 185-193.

Bothast RJ, Schlicher MA (2005). Biotechnological processes for conversion of corn into ethanol. Appl Microbiol Biotechnol 67: 19-25.

Boyle EI, Weng S, Gollub J, Jin H, Botstein D, Cherry JM, Sherlock G (2004). GO::TermFinder—open source software for accessing Gene Ontology information and finding significantly enriched Gene Ontology terms associated with a list of genes. Bioinformatics 20: 3710-3715.

Cankorur-Cetinkaya A, Eraslan S, Kirdar B (2013). Transcriptional remodelling in response to changing copper levels in the Wilson and Menkes disease model of *Saccharomyces cerevisiae*. Mol Biosyst 9: 2889-2908.

Choi GW, Kang HW, Moon, SK (2009). Repeated-batch fermentation using flocculent hybrid, *Saccharomyces cerevisiae* CHFY0321 for efficient production of bioethanol. Appl Microbiol Biotechnol 84: 261-269.

Costenoble R, Valadi H, Gustafsson L, Niklasson C, Franzén CJ (2000). Microaerobic glycerol formation in *Saccharomyces cerevisiae*. Yeast 16: 1483-1495.

Cvijovic M, Olivares-Hernández R, Agren R, Dahr N, Vongsangnak W, Nookaew I, Patil KR, Nielsen J (2010). BioMet Toolbox: genome-wide analysis of metabolism. Nucleic Acids Res 38: 144-149.

De Moraes L, Astolfi-Filho S, Oliver S (1995). Development of yeast strains for the efficient utilisation of starch: evaluation of constructs that express alpha-amylase and glucoamylase separately or as bifunctional fusion proteins. Appl Microbiol Biotechnol 43: 1067-1076.

Elkins JG, Raman B, Keller M (2010). Engineered microbial systems for enhanced conversion of lignocellulosic biomass. Curr Opin Biotechnol 21: 657-662.

Favaro L, Basaglia M, Saayman M, Rose SH, van Zyl WH, Casello S (2010). Engineering amylolytic yeasts for industrial bioethanol production. Chem Eng Transact 20: 97-102.

Gautier L, Cope L, Bolstad BM, Irizarry R (2004). affy—analysis of Affymetrix GeneChip data at the probe level. Bioinformatics 20: 307-315.

Gentleman RC, Carey VJ, Bates DM, Bolstad B, Dettling M, Dudoit S, Ellis B, Gautier L, Ge Y, Gentry J et al. (2004). Bioconductor: Open software development for computational biology and bioinformatics. Genome Biol 5: R80.

Goyal HB, Seal D, Saxena RC (2008). Bio-fuels from thermochemical conversion of renewable resources: a review. Renew Sust Energ Rev 12: 504-517.

Gray KA, Zhao L, Emptage M (2006). Bioethanol. Curr Opin Chem Biol 10: 141-146.

Guimarães PMR, Teixeira JA, Domingues L (2008). Fermentation of high concentrations of lactose to ethanol by engineered flocculent *Saccharomyces cerevisiae*. Biotechnol Lett 30: 1953-1958.

Heux S, Cachon R, Dequin S (2006). Cofactor engineering in *Saccharomyces cerevisiae*: expression of a H_2O-forming NADH oxidase and impact on redox metabolism. Metab Eng 8: 303-314.

Inderwildi OR, King D (2009). Quo vadis biofuels? Energ Environ Sci 2: 343-346.

Karim AS, Curran KA, Alper HS (2013). Characterization of plasmid burden and copy number in *Saccharomyces cerevisiae* for optimization of metabolic engineering applications. FEMS Yeast Res 13: 107-116.

Kasavi C, Eraslan S, Arga K, Toksoy Oner E, Kirdar B (2014). A system based network approach to ethanol tolerance in *Saccharomyces cerevisiae*. BMC Syst Biol 8: 90.

Kim JH, Kim HR, Lim MH, Ko HM, Chin JE, Lee HB, Kim C, Bai S (2010). Construction of a direct starch-fermenting industrial strain of *Saccharomyces cerevisiae* producing glucoamylase, alpha-amylase and debranching enzyme. Biotechnol Lett 32: 713-719.

Li Z, Lee I, Moradi E, Hung NJ, Johnson AW, Marcotte EM (2009). Rational extension of the ribosome biogenesis pathway using network-guided genetics. PLoS Biol 7: e1000213.

Oliveira AP, Patil KR, Nielsen J (2008). Architecture of transcriptional regulatory circuits is knitted over the topology of bio-molecular interaction networks. BMC Syst Biol 2: 17.

Ow DSW, Nissom PM, Philp R, Oh SKW, Yap MGS (2006). Global transcriptional analysis of metabolic burden due to plasmid maintenance in *Escherichia coli* DH5α during batch fermentation. Enzyme Microb Technol 39: 391-398.

Patil KR, Nielsen J (2005). Uncovering transcriptional regulation of metabolism by using metabolic network topology. P Natl Acad Sci USA 102: 2685-2689.

Saeed AI, Bhagabati NK, Braisted JC, Liang W, Sharov V, Howe EA, Li J, Thiagarajan M, White JA, Quackenbush J (2006). TM4 microarray software suite. Method Enzymol 411: 134-193.

Sánchez OJ, Cardona C (2008). Trends in biotechnological production of fuel ethanol from different feedstocks. Bioresour Technol 99: 5270-5295.

Sanchez-Gonzalez Y, Cameleyre X, Molina-Jouve C, Goma G, Alfenore S (2009). Dynamic microbial response under ethanol stress to monitor *Saccharomyces cerevisiae* activity in different initial physiological states. Bioprocess Biosys Eng 32: 459-466.

Shen Y, Zhang Y, Ma T, Bao X, Du F, Zhuang G, Qu Y (2008). Simultaneous saccharification and fermentation of acid-pretreated corncobs with a recombinant *Saccharomyces cerevisiae* expressing beta-glucosidase. Bioresour Technol 99: 5099-5103.

Teixeira MC, Monteiro PT, Guerreiro JF, Gonçalves JP, Mira NP, Dos Santos SC, Cabrito TR, Palma M, Costa C, Francisco AP et al. (2013). The YEASTRACT database: an upgraded information system for the analysis of gene and genomic transcription regulation in *Saccharomyces cerevisiae*. Nucleic Acids Res 42: D161–166.

Toksoy Öner E (2006). Optimization of ethanol production from starch by an amylolytic nuclear petite *Saccharomyces cerevisiae* strain. Yeast 23: 849-856.

Toksoy Öner E, Oliver SG, Kırdar B (2005). Production of ethanol from starch by respiration-deficient recombinant *Saccharomyces cerevisiae*. Appl Environ Microbiol 71: 6443-6445.

Wong DWS, Robertson GH, Lee CC, Wagschal K (2007). Synergistic action of recombinant α-amylase and glucoamylase on the hydrolysis of starch granules. Protein J 26: 159-164.

Yamada R, Bito Y, Adachi T, Tanaka T, Ogino C, Fukuda H, Kondo A (2009). Efficient production of ethanol from raw starch by a mated diploid *Saccharomyces cerevisiae* with integrated α-amylase and glucoamylase genes. Enzyme Microb Technol 44: 344-349.

Yamada R, Yamakawa SI, Tanaka T, Ogino C, Fukuda H, Kondo A (2011). Direct and efficient ethanol production from high-yielding rice using a *Saccharomyces cerevisiae* strain that express amylases. Enzyme Microb Technol 48: 393-396.

Table S1. Strain-significant genes whose expression levels were significantly changed (P < 0.001) in response to the presence of the recombinant vector and the constitutive expression of the amylolytic genes on the plasmid.

ID	Adj. P-value
YGR213C	3.14E-06
YOR134W	4.55E-04
YIL072W	3.85E-05
YBR056W-A	4.77E-07
YNL093W	8.74E-04
YIL073C	7.18E-04
YNR075W	3.33E-04
YLR054C	4.77E-05
YNR064C	9.97E-05
YLR136C	1.46E-04
YJL144W	7.81E-05
YDL114W	1.44E-04
YHR096C	1.41E-04
YAL064W	2.24E-05
YMR316W	3.18E-07
YOL104C	7.93E-04
YGL205W	2.58E-04
YHL012W	6.61E-04
YDR034W-B	2.44E-04
YIL160C	5.51E-04
YOL086W-A	2.80E-07
YNL012W	2.19E-04
YLR213C	9.67E-04
YKL107W	8.18E-04
YBR033W	2.04E-04
YLR121C	1.16E-05
YMR040W	6.31E-06
YDR540C	7.45E-06
YOL016C	3.46E-06
YER184C	5.69E-04
YKL163W	6.81E-04
YLR194C	8.43E-07
YER185W	9.59E-04
YMR085W	2.28E-04
YKL161C	8.86E-06
YKR091W	2.00E-06
YOL155W-A	2.57E-04
YGL156W	9.85E-06
YFR026C	3.04E-05

Table S1. (Continued).

YHR124W	8.17E-04
YCR007C	5.56E-07
YJL116C	3.31E-04
YJR106W	1.98E-04
YMR107W	2.38E-04
YHR138C	4.98E-05
YER039C-A	4.35E-04
YMR034C	4.25E-05
YHR209W	4.99E-05
YOL163W	6.65E-04
YBR045C	3.88E-04
YNR075C-A	8.02E-04
YDR043C	1.64E-05
YLR414C	9.72E-07
YBR005W	4.68E-05
YIL101C	4.67E-04
YGR110W	1.00E-04
YDL024C	2.20E-04
YPL088W	2.65E-05
YMR175W	7.64E-04
YLR099C	2.57E-05
YJR149W	3.56E-04
YOR385W	4.31E-06
YIR028W	1.93E-04
YOR220W	1.56E-05
YCL018W	1.01E-06
YHR139C	5.56E-04
YGL179C	1.15E-04
YGL166W	8.54E-05
YPL156C	2.42E-04
YLR214W	5.27E-04
YIR039C	4.35E-06
YOR289W	1.45E-04
YLL057C	2.90E-04
YMR008C	2.69E-06
YBR295W	2.03E-04
YLR120C	1.19E-06
YOL031C	3.00E-05
YGL251C	8.88E-04
YEL060C	9.07E-06
YMR053C	6.52E-05
YBR072W	2.06E-04
YDL234C	4.49E-05

Table S1. (Continued).

YOL162W	3.02E-04
YJL213W	1.72E-04
YBR047W	5.24E-04
YOR036W	1.10E-06
YOR273C	8.64E-05
YLR149C	1.35E-04
YJR151C	5.95E-04
YFL030W	4.07E-04
YNL092W	3.89E-04
YML130C	1.83E-05
YDR171W	2.06E-04
YPL095C	6.22E-05
YGL126W	1.06E-04
YKR061W	3.47E-05
YJR107W	3.19E-04
YMR184W	1.71E-06
YBR085C-A	5.89E-05
YIL117C	2.01E-05
YBR201W	1.89E-05
YJL057C	7.66E-05
YER175C	3.65E-04
YGR142W	2.45E-04
YML118W	4.75E-06
YHL048W	8.31E-05
YDL027C	9.30E-05
YKL165C	3.01E-07
YJR078W	2.97E-04
YOL091W	4.96E-04
YNL192W	1.46E-05
YJL073W	3.00E-05
YDL199C	4.25E-04
YDL085W	6.29E-05
YCR018C	4.23E-04
YHR030C	3.67E-06
YGR043C	2.44E-05
YOR208W	8.74E-05
YKL073W	1.94E-04
YGR268C	5.99E-06
YJL094C	5.19E-05
YGR032W	3.33E-05
YGL180W	3.41E-04
YER158C	7.69E-05
YMR095C	1.60E-04

Table S1. (Continued).

YKL159C	5.27E-07
YPR079W	1.45E-04
YNR059W	6.74E-05
YER130C	1.43E-05
YJL048C	2.72E-04
YOL083W	4.18E-05
YOR288C	5.88E-06
YLR104W	3.76E-05
YML054C	4.91E-04
YJL153C	4.52E-05
YPL149W	5.70E-05
YAR027W	2.15E-04
YJR019C	9.98E-05
YBR066C	4.49E-05
YJL149W	6.25E-04
YDR358W	5.90E-04
YBR214W	2.16E-05
YLL060C	7.80E-04
YBL078C	8.62E-04
YMR181C	1.16E-04
YKL120W	3.35E-05
YGR161C	1.93E-04
YGL157W	7.96E-06
YNL223W	2.10E-04
YCL049C	2.28E-06
YLL058W	2.07E-04
YIL146C	7.11E-05
YNL015W	2.88E-04
YLR251W	9.99E-04
YDR210W	1.16E-05
YMR020W	1.03E-04
YJL016W	1.76E-04
YDR319C	3.28E-04
YIL001W	3.88E-04
YER035W	1.66E-04
YNR007C	2.06E-04
YPR154W	2.30E-04
YER144C	6.52E-04
YMR271C	9.28E-06
YLR350W	3.55E-05
YBR056W	1.45E-04
YOR034C-A	2.00E-05
YAL028W	6.45E-04

Table S1. (Continued).

YOR035C	2.29E-04
YIL077C	2.03E-04
YOR152C	1.59E-04
YNL208W	1.79E-04
YIL042C	3.62E-04
YDL124W	2.79E-05
YHR102W	2.47E-04
YJL206C	8.80E-05
YDR518W	5.14E-05
YOL014W	7.36E-04
YDR519W	1.30E-05
YGL053W	3.02E-04
YGL009C	6.20E-04
YGL039W	2.27E-04
YDR391C	1.02E-04
YJR142W	6.37E-04
YOR365C	6.47E-04
YDR320C	5.45E-05
YOR192C-C	4.87E-04
YFL031W	2.43E-05
YMR258C	3.66E-04
YDL193W	1.76E-04
YHR106W	7.92E-05
YOR137C	9.02E-05
YNL020C	2.14E-04
YDR411C	1.29E-05
YOL032W	4.57E-05
YNL202W	6.08E-04
YBR269C	2.23E-07
YIR035C	8.27E-04
YPL123C	6.26E-04
YDR503C	5.09E-04
YJL155C	1.40E-04
YGR028W	4.84E-04
YKL151C	2.09E-04
YKR049C	2.39E-04
YIL108W	2.79E-05
YMR191W	4.61E-05
YDR262W	3.03E-04
YHR171W	3.70E-04
YNL289W	3.20E-04
YJL034W	3.57E-06
YGL071W	4.59E-04

Table S1. (Continued).

YNL249C	1.13E-04
YJR008W	4.66E-04
YGL006W	7.43E-05
YDR059C	1.52E-04
YKR076W	7.07E-04
YBR053C	8.00E-06
YNL115C	3.33E-04
YKL206C	1.65E-04
YFR008W	9.02E-06
YBR137W	1.10E-05
YGR168C	7.74E-04
YER150W	8.78E-04
YNR019W	8.89E-04
YGL055W	6.41E-06
YBR071W	2.62E-08
YJR096W	8.06E-05
YGR080W	1.01E-04
YOR321W	1.68E-04
YOL048C	9.18E-05
YHR075C	4.15E-04
YPR117W	3.28E-05
YDR258C	5.23E-04
YGL185C	2.42E-05
YIR002C	6.13E-05
YPL152W	6.60E-04
YEL012W	9.90E-04
YOR020W-A	6.41E-04
YOR329C	2.70E-06
YBR020W	8.56E-05
YOR219C	1.84E-04
YDR400W	6.67E-05
YGR127W	4.18E-04
YPR198W	2.76E-04
YOL013C	1.59E-04
YOL055C	1.53E-04
YNL003C	8.10E-04
YGR284C	2.46E-04
YMR035W	7.82E-04
YHL027W	3.71E-05
YIL154C	6.99E-05
YMR170C	2.83E-04
YDL215C	8.98E-05
YDR533C	2.42E-04

Table S1. (Continued).

YFR039C	8.61E-04
YBL039W-A	1.55E-04
YLR446W	9.45E-04
YIL017C	1.46E-05
YKL065C	3.00E-04
YLR099W-A	2.19E-04
YOR069W	3.93E-04
YDR528W	4.86E-04
YPL109C	3.55E-05
YKL074C	2.71E-05
YHR006W	1.98E-04
YGL059W	9.48E-04
YOR221C	3.14E-05
YNL157W	4.98E-05
YMR096W	4.19E-05
YPL222W	2.26E-04
YAL034C	1.65E-04
YIR017C	7.14E-04
YLR424W	4.78E-04
YNL049C	4.26E-04
YNL293W	1.07E-04
YLR270W	2.83E-04
YFR041C	5.50E-04
YDR539W	1.04E-04
YJR005W	7.20E-05
YPL161C	1.02E-04
YDR423C	9.60E-04
YNL294C	4.41E-04
YLR356W	5.38E-04
YJL020C	2.23E-04
YDL091C	5.38E-04
YLL026W	5.91E-04
YJR036C	6.20E-04
YJL165C	1.52E-04
YNL286W	3.49E-04
YNL044W	2.32E-05
YDR265W	5.17E-04
YDR001C	2.18E-04
YGR189C	1.47E-04
YKL174C	8.82E-04
YOR250C	1.37E-04
YLR100W	1.26E-04
YDR435C	2.49E-04

Table S1. (Continued).

YPL240C	1.35E-04
YDR479C	3.34E-04
YFL042C	2.93E-04
YJR136C	2.16E-04
YKL129C	3.95E-04
YKR046C	7.68E-04
YBL029C-A	7.08E-04
YOR197W	1.61E-05
YNR006W	2.23E-04
YDR055W	2.44E-04
YIR033W	8.77E-04
YLR345W	5.13E-04
YKL188C	2.68E-04
YDL115C	8.24E-04
YPL150W	3.31E-04
YOR209C	3.99E-04
YKL104C	6.49E-04
YDR313C	3.47E-04
YMR087W	3.77E-06
YLR254C	3.52E-04
YBL019W	6.57E-04
YNL040W	6.61E-05
YIR036C	2.75E-04
YHL002W	3.67E-04
YBR149W	3.24E-04
YGL038C	8.21E-04
YBR046C	6.29E-04
YFR042W	2.96E-04
YGR149W	1.97E-04
YOL011W	6.36E-04
YEL020C	6.34E-04
YDR131C	5.42E-04
YOR336W	1.69E-04
YDL149W	8.41E-04
YPL221W	7.76E-05
YDL110C	5.90E-04
YDR538W	6.72E-04
YPR148C	2.55E-05
YKL126W	4.09E-04
YDR242W	1.08E-04
YKR097W	1.53E-04
YIL006W	7.05E-04
YGR136W	5.06E-04

Table S1. (Continued).

YOR213C	7.23E-05
YJL132W	6.60E-04
YLR199C	2.19E-04
YNL241C	9.96E-05
YDL206W	7.39E-04
YNL007C	3.40E-04
YDR122W	7.51E-04
YPL170W	1.58E-04
YOR275C	6.29E-04
YMR160W	1.07E-04
YOR002W	1.34E-04
YLL029W	1.98E-04
YDL020C	5.10E-04
YOL009C	3.66E-04
YPL087W	7.77E-04
YJL141C	6.24E-04
YJL151C	8.08E-05
YKL213C	1.56E-04
YDR436W	4.74E-04
YKL150W	7.04E-04
YGR037C	6.93E-05
YBR036C	6.58E-04
YKL012W	9.04E-05
YPL249C	6.91E-05
YKR003W	3.15E-05
YPR147C	4.69E-04
YLR256W	6.22E-04
YDR295C	5.86E-04
YPL001W	9.07E-05
YPL052W	1.47E-04
YCL043C	1.33E-04
YML013W	3.99E-05
YAL002W	2.54E-04
YDR141C	1.00E-04
YLR216C	7.61E-04
YPL120W	1.98E-04
YMR022W	1.57E-04
YBR176W	4.07E-04
YOR299W	3.27E-04
YOL002C	1.99E-04
YDR525W-A	3.54E-04
YKL010C	4.44E-04
YMR295C	8.76E-04

Table S1. (Continued).

YBR273C	3.27E-04
YCL047C	9.04E-04
YKL142W	7.19E-04
YPL085W	1.11E-04
YLL039C	4.50E-04
YMR315W	7.93E-04
YML057W	1.09E-04
YJL163C	7.77E-04
YHR208W	7.99E-05
YGL242C	9.75E-04
YPL100W	1.13E-04
YMR238W	4.08E-05
YLR028C	1.03E-04
YHR134W	8.63E-04
YMR173W	7.09E-04
YMR176W	4.64E-05
YDR166C	2.58E-05
YKL193C	6.26E-04
YOR236W	4.78E-04
YKL157W	1.84E-04
YMR025W	5.62E-04
YLR371W	6.97E-04
YJR138W	5.84E-04
YEL059C-A	4.64E-05
YJL171C	8.71E-06
YNR039C	1.97E-04
YNL011C	6.96E-04
YLR207W	7.02E-04
YJL091C	9.64E-04
YJL084C	2.30E-04
YBR101C	2.43E-04
YDR129C	3.42E-04
YMR013C	1.94E-04
YHR017W	4.51E-04
YCL040W	7.51E-05
YKL013C	5.35E-04
YPL159C	7.96E-04
YGL141W	7.08E-05
YJL159W	1.11E-06
YMR097C	3.82E-04
YBR126C	2.00E-04
YLR292C	4.58E-05
YJL079C	9.78E-05

Table S1. (Continued).

YDL125C	7.82E-05
YMR054W	1.33E-04
YBL088C	1.03E-04
YOR099W	2.81E-04
YCR036W	4.26E-04
YDR078C	4.42E-04
YNL161W	6.77E-04
YDR434W	3.64E-06
YPL071C	3.31E-04
YDR305C	5.60E-05
YGL208W	4.70E-04
YBR170C	3.21E-04
YKL007W	5.64E-05
YIL034C	8.61E-05
YHR190W	3.41E-04
YGL057C	2.71E-04
YLR367W	5.05E-04
YHR188C	5.48E-04
YKL124W	2.62E-04
YGL128C	2.30E-04
YEL058W	7.68E-04
YPR172W	7.47E-04
YGR255C	7.65E-04
YDR077W	3.25E-04
YDL123W	4.69E-04
YNL079C	5.32E-04
YDR407C	5.37E-04
YOR238W	1.63E-04
YBR109C	3.51E-05
YML070W	1.02E-04
YJL167W	2.23E-05
YBR016W	1.76E-04
YCR009C	9.70E-04
YGL167C	4.12E-05
YMR122W-A	3.51E-04
YAL016W	5.73E-04
YLR179C	4.01E-04
YDL012C	4.34E-04
YIR038C	5.24E-04
YMR226C	1.08E-04
YMR220W	4.07E-04
YGR010W	6.36E-04
YER136W	1.31E-04

Table S1. (Continued).

YML074C	9.35E-04
YLR390W-A	4.81E-04
YLL040C	9.82E-04
YBR080C	7.61E-05
YOR198C	6.79E-04
YLR188W	8.90E-05
YML028W	3.66E-04
YGR217W	2.37E-04
YDR189W	5.28E-05
YJR024C	8.76E-07
YGR235C	6.42E-04
YBR173C	8.02E-04
YPR165W	2.65E-05
YPR075C	7.67E-04
YGR244C	9.91E-04
YAL007C	4.58E-04
YPL031C	4.39E-04
YAL051W	2.63E-04
YLR429W	7.91E-04
YPL154C	1.53E-04
YDR099W	1.94E-04
YMR092C	4.09E-04
YOR254C	5.89E-04
YDL029W	6.93E-04
YNL118C	6.42E-04
YLR085C	7.76E-04
YKL039W	2.06E-04
YPL028W	1.29E-04
YMR026C	9.24E-05
YPL188W	5.59E-05
YKL182W	1.39E-04
YPR159W	9.32E-04
YNL138W	1.49E-05
YDR073W	6.77E-04
YHR098C	8.34E-05
YPL218W	2.55E-04
YEL031W	8.01E-04
YNL055C	2.61E-04
YDR155C	7.63E-07
YBL105C	5.59E-05
YIL041W	4.94E-04
YDR164C	6.08E-04
YML012W	4.74E-04

Table S1. (Continued).

YGR157W	4.46E-04
YLR355C	5.30E-04
YAL001C	8.23E-04
YPL232W	6.71E-04
YPL115C	6.41E-04
YNL212W	1.49E-04
YER094C	4.82E-04
YPL078C	7.36E-04
YLR354C	7.86E-04
YKL145W	2.91E-04
YLR192C	8.02E-04
YDL126C	7.77E-04
YOR312C	7.41E-05
YJR123W	3.04E-04
YDR382W	3.65E-04
YLR090W	9.33E-04
YER125W	1.21E-05
YHR007C	3.70E-04
YLR060W	5.38E-04
YDR025W	7.35E-04
YGR155W	1.71E-04
YJL136C	3.27E-04
YER026C	8.80E-04
YEL027W	2.52E-04
YBR078W	3.64E-05
YBR189W	3.62E-04
YOL039W	8.11E-04
YOR276W	5.56E-04
YHR181W	8.46E-05
YDL182W	2.31E-04
YLR335W	3.24E-04
YMR177W	4.27E-04
YBR067C	8.28E-04
YDR023W	3.64E-04
YOR303W	6.10E-04
YER031C	7.74E-04
YNL001W	3.57E-04
YDR182W	2.70E-04
YKL144C	2.01E-05
YIL069C	2.00E-06
YGL008C	7.13E-04
YHR026W	1.98E-04
YML085C	3.78E-04

Table S1. (Continued).

YOL123W	5.20E-04
YKL035W	8.26E-04
YFR038W	6.16E-04
YGR095C	7.71E-06
YMR235C	6.13E-04
YPL234C	7.94E-04
YMR285C	8.89E-04
YKR026C	8.89E-04
YGL106W	8.89E-04
YOL058W	7.17E-04
YBR029C	1.42E-04
YBL087C	1.97E-04
YOL103W	3.65E-05
YNL113W	8.75E-04
YNL169C	7.60E-04
YOR308C	5.76E-04
YOR175C	7.18E-04
YNL292W	8.28E-04
YPL158C	4.90E-04
YBR283C	2.52E-04
YHR133C	6.20E-05
YLR372W	5.15E-06
YBR074W	9.50E-04
YNR021W	4.84E-04
YLR186W	3.60E-04
YKL130C	9.51E-04
YPR113W	7.05E-04
YKL085W	1.86E-04
YNL220W	2.80E-04
YCR034W	2.46E-04
YDR347W	7.59E-04
YOR168W	5.28E-04
YOR021C	4.64E-04
YPL063W	8.54E-04
YDR404C	2.79E-04
YAR007C	7.32E-04
YKL081W	1.24E-05
YHR013C	3.59E-04
YCR077C	2.10E-05
YLR328W	9.54E-04
YNL153C	7.14E-04
YGL021W	9.54E-04
YGR215W	1.31E-05

Table S1. (Continued).

YNL155W	5.47E-04
YMR203W	7.06E-04
YNL232W	9.13E-04
YNL181W	2.14E-04
YMR277W	1.79E-04
YML035C	5.61E-04
YGR061C	5.43E-04
YEL038W	3.36E-04
YLR020C	2.71E-04
YLR175W	4.49E-04
YDL208W	9.36E-05
YML125C	1.50E-04
YHR005C-A	7.71E-04
YDL160C	5.05E-04
YMR193W	6.33E-04
YBR265W	4.61E-05
YGL120C	4.29E-04
YGR074W	5.32E-04
YML053C	9.43E-04
YPR100W	1.74E-04
YER146W	3.93E-04
YJR010W	1.66E-04
YEL017W	2.47E-06
YOR310C	5.03E-04
YHL001W	5.96E-05
YDR345C	5.88E-07
YKL175W	4.00E-04
YOL077C	7.77E-04
YDR207C	2.99E-04
YJR015W	7.66E-04
YGR140W	1.00E-05
YJR056C	4.83E-04
YDR079W	7.85E-04
YPR149W	1.15E-04
YHL031C	7.97E-05
YDL213C	5.20E-04
YNL268W	8.02E-04
YHR061C	4.77E-05
YDR054C	2.03E-04
YNL102W	1.86E-04
YHR068W	1.40E-04
YPL211W	9.01E-05
YPR120C	1.90E-04

Table S1. (Continued).

YJL183W	5.59E-07
YIL118W	1.54E-04
YEL020W-A	9.56E-04
YHR089C	9.24E-04
YLR197W	8.53E-04
YOR145C	4.27E-05
YOR001W	6.27E-04
YNL132W	4.92E-04
YMR229C	5.74E-04
YNL058C	2.28E-04
YDL164C	6.15E-05
YOL143C	2.23E-04
YML009C	7.81E-04
YHR144C	7.64E-04
YJR143C	9.48E-04
YDL202W	4.27E-05
YGL010W	8.97E-05
YGR158C	7.91E-04
YGL097W	1.12E-04
YGL099W	7.33E-04
YEL042W	7.50E-05
YHR088W	8.82E-04
YMR076C	8.83E-04
YJL104W	1.99E-04
YHR128W	8.72E-04
YOL125W	3.56E-05
YBL098W	4.48E-04
YPR071W	8.69E-04
YDR280W	4.73E-04
YJL087C	4.52E-04
YDL014W	8.92E-05
YDR146C	2.14E-04
YMR241W	1.88E-05
YBR218C	3.36E-04
YDR245W	1.39E-04
YOR252W	7.57E-04
YNR017W	1.74E-04
YPL263C	4.13E-04
YMR300C	2.41E-05
YBR154C	3.99E-04
YOR136W	3.92E-05
YDR046C	4.36E-04
YDR322W	1.33E-04

Table S1. (Continued).

YKL154W	7.54E-05
YDR267C	7.55E-04
YMR145C	4.11E-04
YJL096W	9.21E-04
YGL139W	2.98E-04
YER029C	4.78E-04
YKL009W	2.85E-04
YBL071W-A	5.89E-04
YDL209C	6.52E-04
YLR312W-A	2.58E-04
YPR143W	9.65E-05
YPL012W	7.65E-04
YLR129W	3.76E-07
YER113C	9.90E-04
YER016W	3.94E-04
YJR070C	6.61E-04
YML096W	7.93E-04
YER032W	3.89E-04
YCR003W	2.73E-04
YDL105W	4.71E-04
YHR062C	6.81E-04
YOL056W	6.00E-04
YGR191W	6.13E-05
YKL166C	2.92E-04
YJL208C	3.84E-05
YNL129W	3.42E-05
YPR041W	4.80E-05
YHR196W	4.41E-04
YDR393W	8.16E-05
YOR187W	1.48E-05
YPL227C	5.37E-06
YGL040C	8.74E-04
YNL264C	9.76E-04
YOL140W	2.18E-04
YKR072C	3.16E-04
YDR337W	2.88E-04
YER095W	9.73E-04
YMR215W	4.31E-04
YBR187W	3.04E-04
YDR033W	8.07E-04
YOL115W	8.31E-04
YGR238C	9.88E-04
YDR361C	6.77E-05

Table S1. (Continued).

YOR229W	1.00E-04
YDR354W	1.40E-04
YIL053W	1.69E-05
YNL262W	7.11E-05
YPR060C	3.96E-04
YIL127C	5.14E-04
YGL213C	6.74E-04
YGR152C	1.95E-04
YLR009W	6.25E-04
YIL140W	2.94E-04
YMR070W	7.27E-04
YEL063C	9.31E-04
YNL151C	8.94E-05
YGR266W	1.36E-05
YOR272W	8.75E-04
YMR243C	9.70E-04
YGR251W	8.04E-04
YLR154C	6.46E-04
YDL227C	4.65E-06
YJL088W	7.94E-04
YOR071C	7.28E-04
YPL043W	6.49E-04
YPL086C	9.48E-04
YPL265W	7.46E-04
YBR142W	5.27E-04
YFL004W	5.34E-04
YOR222W	1.34E-04
YHR052W	3.35E-05
YPL026C	7.62E-04
YLR326W	2.93E-04
YNL075W	2.38E-04
YNL197C	1.06E-04
YLR409C	4.20E-04
YLR196W	4.08E-04
YKL029C	9.83E-04
YKL216W	4.70E-04
YPL126W	6.07E-04
YLR049C	3.00E-04
YOR302W	7.44E-04
YLR222C	4.28E-04
YCL054W	5.11E-04
YIL165C	8.07E-04
YGR082W	8.56E-04

Table S1. (Continued).

YDR299W	7.00E-05
YDR449C	2.79E-04
YNL252C	4.98E-04
YCR087C-A	1.61E-05
YHR033W	2.74E-04
YIL093C	8.99E-05
YCL058C	6.92E-04
YLR437C	9.05E-04
YDR075W	4.02E-07
YPL207W	9.39E-04
YOR073W	7.42E-04
YBR268W	5.48E-05
YER002W	3.45E-04
YLR420W	5.04E-05
YGR187C	4.83E-04
YPL132W	7.45E-04
YBR247C	4.48E-04
YGR078C	2.09E-05
YGR169C-A	2.00E-04
YNL301C	5.77E-04
YBR291C	2.07E-04
YIL162W	5.02E-05
YJL198W	6.32E-04
YKL099C	2.22E-04
YIL091C	9.57E-04
YEL036C	5.80E-04
YIL103W	5.47E-04
YCL063W	1.22E-04
YPR144C	7.85E-04
YOR340C	2.84E-04
YGR109C	6.19E-04
YBL032W	3.04E-05
YIL009W	8.37E-04
YJR097W	8.48E-04
YBR028C	2.17E-05
YPL157W	8.10E-04
YER001W	1.74E-04
YGR245C	1.16E-04
YJL186W	2.31E-04
YDR297W	5.19E-05
YLR032W	4.61E-04
YIL132C	9.74E-04
YGR031W	5.24E-04
YLR183C	6.54E-04
YIL070C	3.71E-04

Table S1. (Continued).

YLR008C	1.95E-06
YJL134W	5.23E-05
YDL148C	4.58E-04
YBL009W	3.88E-05
YNR013C	6.98E-04
YML058W-A	5.73E-04
YLR084C	9.31E-04
YIL020C	4.47E-04
YOL052C	6.51E-05
YDR398W	3.42E-04
YLL008W	6.62E-04
YNL182C	3.57E-04
YMR195W	1.13E-04
YEL017C-A	4.18E-04
YER064C	3.86E-05
YNL068C	4.48E-04
YOR004W	1.53E-04
YNR053C	3.42E-04
YCL024W	1.51E-04
YNR028W	9.32E-04
YDR527W	3.48E-04
YBR271W	2.93E-05
YLL013C	4.46E-05
YOR119C	3.93E-04
YLL009C	6.45E-04
YDL049C	1.30E-04
YNL072W	1.87E-04
YMR011W	1.74E-04
YLL011W	1.64E-04
YFR053C	4.07E-06
YGR103W	1.38E-04
YNL037C	2.95E-04
YGR030C	3.96E-04
YOR095C	4.78E-05
YMR231W	3.21E-05
YGR159C	9.98E-04
YJL122W	1.31E-04
YGL029W	2.05E-04
YBL028C	1.81E-04
YIL164C	9.06E-04
YML018C	2.07E-04
YKR060W	2.83E-04
YGR280C	1.95E-04
YNL141W	6.30E-04
YNL024C	2.86E-04

Table S1. (Continued).

YPL193W	7.08E-04
YGR205W	5.85E-04
YML052W	3.25E-04
YCR072C	3.97E-04
YLR023C	2.63E-04
YMR290C	2.77E-04
YHL016C	9.23E-05
YHR049W	3.64E-04
YLR068W	1.06E-04
YDR083W	3.32E-04
YKL096W	5.38E-04
YBL069W	3.68E-05
YOL028C	2.58E-04
YJL033W	3.38E-04
YLR407W	2.43E-04
YIL158W	6.08E-05
YAL025C	3.26E-04
YKL109W	3.45E-04
YIL019W	7.55E-04
YLR401C	6.86E-04
YAL059W	1.38E-04
YOL124C	1.43E-04
YPR119W	3.15E-04
YDL241W	7.02E-04
YGL209W	6.30E-04
YDR111C	2.95E-04
YGR109W-B	5.08E-04
YGR079W	3.80E-04
YOR342C	2.48E-04
YJL196C	4.53E-06
YHL024W	8.35E-04
YOR161C	1.99E-05
YCR061W	9.69E-04
YNR009W	5.75E-04
YPL279C	4.22E-06
YOR287C	7.22E-05
YGR234W	1.14E-04
YBR085W	2.06E-04
YDL205C	5.40E-04
YNL173C	5.01E-06
YJL218W	3.85E-04
YFR015C	2.61E-04
YJR048W	9.87E-04
YPL092W	2.35E-04
YDR481C	7.65E-05

Table S1. (Continued).

YMR303C	3.03E-04
YOR101W	2.73E-05
YLR413W	6.03E-05
YPL189C-A	8.63E-04
YLL061W	3.05E-04
YHL026C	2.91E-04
YAL067C	9.16E-04
YPR002W	4.00E-05
YJR147W	2.92E-04
YER187W	9.62E-05
YOL136C	1.79E-05
YLR063W	4.84E-04
YIL011W	6.87E-04
YGL035C	2.53E-04
YNL112W	6.21E-04
YNL142W	8.60E-05
YGL162W	5.92E-04
YLR130C	3.12E-05
YDR384C	1.68E-04
YEL039C	9.67E-05
YBR069C	6.84E-05
YLL055W	3.41E-04
YGR243W	7.60E-04
YER053C-A	9.16E-04
YOL155C	1.43E-06
YNL065W	4.85E-04
YBL029W	2.92E-05
YBL042C	1.32E-04
YOR348C	3.74E-04
YLR267W	8.46E-04
YGR286C	1.04E-04
YAR068W	4.47E-05
YJL212C	3.33E-06
YJL170C	6.83E-04
YDR277C	2.90E-05
YBR050C	2.42E-04
YBR092C	6.87E-06
YGL255W	1.44E-05
YHR092C	1.06E-05
YKR075C	5.41E-05
YHR214C-D	6.50E-04
YOL154W	1.94E-04
YOR378W	1.30E-05
YOR100C	2.30E-04
YPR194C	1.30E-06

Table S2. Aeration-significant genes whose expression levels were significantly changed (P < 0.001) in response to oxygen limitation.

ID	Adj. P-value
YML037C	2.27E-04
YOL084W	2.29E-04
YDL222C	5.17E-04
YLR108C	9.88E-05
YDR223W	5.96E-04
YJL108C	3.46E-04
YFR035C	4.10E-05
YCL001W-A	7.65E-04
YOL101C	5.61E-05
YDR317W	1.33E-04
YBR148W	6.54E-04
YGR035W-A	8.39E-04
YOR365C	6.19E-05
YNL036W	4.78E-07
YGR240C-A	6.14E-04
YKR053C	8.00E-04
YLL042C	1.55E-04
YIR015W	4.88E-04
YIR028W	5.11E-04
YGR142W	1.75E-04
YOL162W	3.72E-04
YLL055W	9.68E-04
YLR411W	1.95E-04
YOR349W	3.39E-05
YPL192C	5.09E-04
YGL051W	1.05E-04
YPR193C	9.53E-05
YLR024C	1.79E-04
YDR009W	5.71E-04
YJL056C	1.61E-04
YBR244W	2.70E-04
YJL106W	7.07E-04
YCL021W-A	7.45E-04
YLR174W	6.42E-04
YDR273W	9.74E-04
YOL151W	1.62E-04
YJL132W	3.37E-05
YPL258C	3.73E-04
YGR131W	4.81E-04
YJR039W	6.97E-04

Table S2. (Continued).

YOL105C	4.11E-04
YMR190C	4.78E-04
YCR106W	5.17E-04
YCR020C	8.72E-04
YDR144C	1.14E-05
YOL013W-B	6.89E-04
YPR026W	2.27E-04
YPL174C	7.24E-04
YEL023C	3.04E-04
YFL010W-A	1.42E-05
YDL206W	9.91E-05
YOL113W	1.29E-04
YLR084C	5.84E-04
YBR150C	7.29E-04
YMR287C	8.11E-04
YJL206C	1.10E-04
YOL164W	5.16E-04
YHR099W	7.31E-04
YJL163C	5.79E-05
YGR043C	1.06E-04
YLR424W	1.80E-04
YJR036C	2.12E-04
YHR171W	3.48E-04
YPL016W	9.23E-04
YKL161C	7.02E-04
YLR138W	5.50E-04
YBR020W	6.17E-05
YER164W	8.56E-04
YGR188C	8.80E-04
YIR031C	3.70E-04
YGL176C	2.72E-04
YGR014W	9.91E-04
YPL024W	5.77E-05
YHL030W	4.70E-04
YPR002W	5.13E-04
YHL036W	9.25E-04
YOR109W	4.67E-04
YIR033W	3.36E-04
YDL239C	8.57E-04
YOR249C	1.92E-04
YDR334W	2.30E-05
YPR121W	1.39E-04
YNL008C	2.23E-04

Table S2. (Continued).

YBR068C	2.36E-04
YML059C	1.36E-04
YKR091W	2.72E-04
YKL149C	1.08E-04
YKL105C	3.34E-04
YOR161C	1.77E-04
YIL140W	1.69E-04
YBR133C	5.45E-04
YHR155W	8.48E-05
YPL109C	3.48E-05
YPL005W	2.99E-04
YHR120W	6.35E-04
YER173W	8.62E-05
YGL197W	9.21E-04
YJL154C	1.23E-04
YJL093C	5.97E-04
YDR104C	6.18E-04
YKR031C	2.80E-04
YNL273W	7.33E-04
YKR027W	2.71E-04
YNL029C	7.55E-04
YDL085W	8.35E-04
YAL058W	3.23E-04
YDR078C	6.68E-05
YOL032W	1.71E-04
YMR013C	3.94E-05
YDL020C	2.50E-04
YOL086W-A	1.88E-04
YIL146C	5.01E-04
YNL329C	3.75E-04
YER066W	6.46E-04
YBR235W	3.32E-04
YMR275C	3.04E-04
YDL200C	8.04E-05
YLR454W	1.61E-04
YAR019C	5.99E-04
YDR150W	5.95E-05
YDR128W	6.68E-05
YDR479C	3.53E-04
YIL017C	2.40E-05
YOR054C	8.72E-04
YIL147C	7.79E-05
YDR533C	4.42E-04

Table S2. (Continued).

YLR103C	1.55E-04
YDR027C	1.88E-04
YPL150W	2.98E-04
YGL006W	2.62E-04
YMR145C	2.50E-04
YML051W	3.56E-04
YIL149C	2.73E-04
YLR004C	5.42E-04
YPL120W	8.40E-05
YMR119W	4.06E-04
YGR217W	1.84E-05
YDR436W	2.93E-04
YJL155C	6.84E-04
YLR383W	1.83E-04
YDR239C	5.21E-04
YDR520C	8.31E-04
YGL027C	3.78E-04
YGL247W	8.25E-04
YBL088C	2.63E-05
YFL034W	6.83E-04
YKL165C	8.80E-06
YDR313C	3.95E-04
YOR336W	1.62E-04
YDR490C	8.69E-04
YPR117W	1.14E-04
YPL222W	4.90E-04
YDR118W	1.84E-04
YOR328W	8.18E-05
YIL117C	7.34E-04
YBL019W	8.32E-04
YMR036C	2.85E-04
YOR219C	6.46E-04
YFL041W	2.51E-04
YKL171W	6.86E-04
YDR131C	6.27E-04
YKR010C	8.56E-04
YAL051W	2.12E-05
YDR135C	1.14E-04
YNL249C	6.20E-04
YGR196C	6.56E-04
YJR096W	3.61E-04
YIL063C	1.93E-04
YOR076C	6.44E-04

Table S2. (Continued).

YBR275C	2.64E-04
YKL090W	8.45E-04
YBR074W	1.39E-04
YMR162C	6.44E-04
YGR258C	4.56E-04
YBR081C	1.74E-04
YMR160W	1.27E-04
YGL160W	8.92E-04
YLR371W	3.70E-04
YJL112W	2.72E-04
YFL025C	5.01E-04
YGL229C	5.78E-04
YKL012W	7.60E-05
YPL085W	7.34E-05
YMR054W	5.49E-05
YLL048C	1.39E-04
YDR407C	1.29E-04
YMR025W	3.25E-04
YMR257C	1.40E-04
YBL075C	3.57E-04
YOR321W	9.49E-04
YIL036W	5.75E-04
YEL059C-A	2.90E-05
YLR006C	6.11E-04
YOL048C	5.58E-04
YGL233W	4.96E-04
YLR417W	4.74E-04
YLR442C	2.69E-04
YKR003W	3.42E-05
YNL192W	7.51E-04
YCR011C	6.50E-04
YNL251C	8.03E-04
YNL040W	1.53E-04
YEL025C	8.38E-04
YLR095C	2.77E-04
YMR060C	3.08E-04
YGL023C	4.12E-05
YNL291C	5.72E-04
YJR059W	1.97E-04
YJL165C	5.78E-04
YPR091C	8.72E-04
YPR155C	7.23E-05
YGL062W	2.45E-04

Table S2. (Continued).

YLR071C	5.77E-04
YOL063C	5.39E-04
YBR170C	1.84E-04
YJR046W	2.34E-04
YAL002W	3.14E-04
YIL139C	4.35E-04
YER007W	4.54E-04
YLR324W	5.36E-04
YBR281C	3.86E-04
YLR389C	2.48E-04
YHR028C	6.88E-04
YIR002C	5.93E-04
YFR048W	3.94E-04
YGL133W	1.91E-04
YLR207W	7.36E-04
YMR086W	2.61E-04
YOR299W	4.95E-04
YKL124W	1.70E-04
YLR189C	6.61E-04
YPR029C	1.12E-04
YMR192W	8.28E-04
YJL062W	7.99E-04
YOL081W	3.99E-04
YFR013W	3.98E-04
YBR229C	1.81E-04
YML118W	5.56E-04
YAL026C	6.99E-04
YPL221W	2.97E-04
YPL176C	1.45E-04
YHR017W	5.89E-04
YDL215C	9.11E-04
YPL240C	8.06E-04
YNL293W	8.57E-04
YDR294C	2.72E-04
YDL044C	1.47E-04
YHR030C	3.82E-04
YOR086C	4.17E-04
YNL241C	3.83E-04
YKL010C	9.35E-04
YKL015W	4.33E-04
YFR031C	3.65E-04
YIL108W	6.88E-04
YMR126C	9.17E-04

Table S2. (Continued).

YOR034C-A	8.69E-04
YDL174C	5.51E-05
YBR227C	3.19E-04
YPL097W	4.58E-04
YMR176W	1.02E-04
YBR003W	9.25E-04
YGL067W	9.44E-05
YNL212W	8.17E-06
YFR038W	1.91E-04
YNL157W	6.96E-04
YHR188C	7.83E-04
YPL100W	3.35E-04
YGL010W	3.63E-04
YLR135W	2.26E-04
YNR055C	8.51E-04
YNR041C	6.18E-04
YGL057C	5.21E-04
YLL040C	9.60E-04
YFL009W	4.24E-04
YDR242W	9.81E-04
YNL215W	4.85E-04
YPL115C	6.91E-05
YBR163W	9.86E-04
YAL001C	1.06E-04
YMR238W	2.06E-04
YDL013W	4.75E-04
YGR210C	8.84E-04
YLR188W	1.11E-04
YDR307W	3.75E-04
YKL039W	1.59E-04
YGR157W	8.93E-05
YBL067C	3.81E-04
YDR434W	1.66E-05
YGL167C	1.22E-04
YDR227W	9.80E-04
YGL141W	5.09E-04
YIL005W	6.45E-05
YLR259C	4.48E-04
YNL118C	9.79E-04
YGL086W	9.19E-04
YDL164C	9.93E-04
YLR109W	1.94E-04
YHR098C	1.41E-04

Table S2. (Continued).

YJR040W	5.12E-04
YOR371C	4.16E-04
YMR087W	4.14E-04
YMR026C	4.36E-04
YBL105C	1.41E-04
YGR140W	4.00E-04
YLR044C	4.22E-04
YML001W	7.88E-04
YER125W	2.39E-04
YDR155C	4.03E-04
YJR024C	8.90E-04
YDR224C	4.86E-04
YLR180W	9.48E-04
YGL105W	9.31E-04
YKL096W-A	7.37E-05
YGR155W	2.69E-04
YIL069C	1.30E-05
YNL307C	7.33E-04
YEL027W	3.01E-04
YHR181W	1.85E-04
YJL183W	3.13E-05
YNL004W	4.02E-04
YBR162C	7.37E-04
YLR150W	5.46E-04
YNL244C	8.33E-04
YDR502C	3.56E-04
YBR071W	6.33E-06
YER052C	9.67E-04
YOR157C	5.42E-04
YMR152W	2.83E-04
YOR247W	8.74E-04
YBR078W	1.46E-05
YNL001W	4.92E-04
YBR177C	8.67E-04
YPR165W	8.26E-05
YBR265W	3.79E-04
YJL001W	8.69E-04
YHR007C	4.67E-05
YEL017W	2.27E-05
YPL031C	8.90E-04
YGR262C	3.74E-04
YPL066W	4.15E-04
YCR092C	1.87E-04

Table S2. (Continued).

YJR010W	9.39E-04
YLR192C	7.12E-05
YGR279C	5.75E-05
YLR008C	1.54E-04
YFL005W	5.16E-04
YCR034W	6.39E-04
YDR404C	7.37E-04
YBR067C	3.04E-04
YDR397C	6.26E-05
YKL117W	7.06E-04
YNL220W	6.52E-04
YBR109C	8.81E-05
YDR487C	3.49E-04
YDL226C	9.45E-04
YAL009W	2.20E-05
YML085C	2.70E-04
YJL171C	5.00E-05
YOR332W	4.15E-05
YOL058W	5.75E-04
YIL118W	8.81E-04
YOL125W	2.78E-04
YGR026W	2.46E-04
YOR089C	7.30E-04
YBR127C	2.81E-04
YDL111C	6.24E-04
YMR235C	3.83E-04
YER099C	6.82E-04
YOR317W	3.14E-04
YER120W	3.14E-04
YCR077C	3.65E-05
YDR073W	2.35E-04
YKL040C	5.11E-05
YDR077W	5.68E-04
YGR086C	5.58E-04
YPR082C	1.43E-04
YDR099W	1.23E-04
YOR279C	8.12E-04
YAR015W	3.47E-04
YHR013C	5.39E-04
YPL211W	3.60E-04
YGL128C	4.28E-04
YNL010W	7.46E-04
YDR245W	7.75E-04

Table S2. (Continued).

YDR174W	9.71E-04
YDL166C	8.68E-04
YLR129W	2.83E-06
YDR092W	1.51E-04
YPR041W	3.87E-04
YMR177W	6.31E-05
YOR303W	1.30E-04
YDR075W	8.04E-06
YLR244C	8.73E-04
YIR037W	2.97E-04
YGR207C	4.91E-04
YBR271W	9.17E-04
YPR113W	5.17E-04
YPR075C	3.64E-04
YOL008W	3.29E-04
YNL173C	8.81E-04
YNL151C	7.43E-04
YGL087C	6.08E-04
YPL129W	9.82E-04
YGR180C	3.12E-05
YIL114C	6.01E-04
YBR029C	4.89E-05
YGR020C	6.41E-04
YGL120C	5.63E-04
YMR210W	1.39E-04
YCL012C	3.20E-04
YOR039W	2.93E-04
YBR171W	3.48E-04
YEL051W	5.41E-06
YIL034C	9.80E-05
YFR053C	1.11E-04
YMR079W	1.67E-04
YOL147C	3.66E-04
YGR078C	2.72E-04
YDR354W	7.07E-04
YDL170W	6.69E-04
YBR002C	6.91E-04
YDR368W	3.99E-05
YDL014W	1.98E-04
YLR262C	9.98E-04
YML078W	7.92E-05
YBR249C	2.60E-04
YGL219C	5.08E-04

Table S2. (Continued).

YFL028C	8.96E-04
YCR035C	2.62E-04
YKL166C	8.45E-04
YNL300W	1.74E-04
YKL007W	3.89E-05
YNR061C	3.33E-04
YEL047C	5.63E-05
YDL123W	2.19E-04
YLR420W	3.63E-04
YCR087C-A	1.01E-04
YDR299W	4.20E-04
YPR063C	6.04E-04
YDR054C	2.07E-04
YBR035C	8.71E-05
YNL113W	1.66E-04
YDR280W	6.72E-04
YCL050C	5.51E-05
YIL154C	4.36E-04
YCL063W	8.64E-04
YNL058C	2.34E-04
YOR145C	4.08E-05
YML053C	5.17E-04
YNR018W	9.36E-04
YDR322W	1.99E-04
YIR026C	3.94E-04
YGL169W	7.82E-04
YKL159C	2.20E-05
YFR007W	7.33E-04
YJR056C	3.38E-04
YPR143W	1.43E-04
YHR187W	4.81E-05
YMR272C	9.74E-04
YJL217W	3.33E-04
YGL018C	3.22E-04
YPL117C	6.03E-04
YOR283W	6.28E-04
YNL211C	7.61E-04
YLR201C	8.27E-05
YHR175W	4.47E-04
YGR095C	5.21E-07
YMR195W	6.97E-04
YGR080W	5.30E-04
YIL083C	2.28E-04

Table S2. (Continued).

YOL030W	5.97E-04
YOR252W	6.62E-04
YLR268W	8.42E-05
YHR088W	6.66E-04
YFR008W	4.69E-05
YPR071W	6.57E-04
YHR061C	2.35E-05
YMR030W	5.10E-04
YJL208C	4.52E-05
YOR304C-A	1.53E-04
YFL034C-B	8.18E-04
YGL058W	1.14E-04
YJL052W	1.20E-04
YOL155C	2.35E-04
YDR055W	3.33E-04
YKL103C	6.54E-04
YMR178W	9.65E-04
YJR103W	7.76E-05
YER126C	2.94E-04
YOR213C	6.20E-05
YOR295W	6.84E-04
YNR027W	2.41E-04
YER134C	9.50E-04
YLR275W	4.28E-04
YDR345C	1.38E-07
YLR284C	1.85E-04
YDL160C	8.47E-05
YHR052W	4.03E-05
YOL140W	1.51E-04
YLR243W	2.34E-04
YGR158C	2.43E-04
YOR229W	5.83E-05
YDR033W	4.65E-04
YDL043C	3.23E-05
YNL158W	1.32E-04
YNR007C	8.95E-04
YER064C	7.71E-05
YBR006W	1.01E-04
YGL029W	5.90E-04
YLR068W	4.23E-04
YKL144C	2.93E-07
YLL025W	5.12E-05
YGR161C	9.05E-04

Table S2. (Continued).

YLR009W	3.20E-04
YEL073C	4.73E-04
YHR167W	5.98E-04
YCL031C	6.55E-04
YOR319W	8.39E-05
YER100W	5.82E-05
YNL190W	1.82E-04
YJL122W	2.63E-04
YOL143C	3.21E-05
YNL075W	1.29E-04
YNL264C	2.91E-04
YOR315W	2.76E-04
YKL099C	1.86E-04
YNL301C	4.49E-04
YHR059W	2.97E-04
YOR101W	2.87E-04
YKL068W-A	3.57E-04
YOR344C	3.61E-04
YMR011W	2.01E-04
YCL049C	5.48E-06
YJL079C	5.84E-06
YNL111C	4.29E-04
YGR049W	5.19E-04
YGR138C	1.02E-04
YAR028W	1.17E-04
YOR287C	2.79E-04
YIL111W	7.08E-04
YER139C	7.38E-04
YKL216W	1.45E-04
YMR271C	1.14E-05
YGR036C	8.76E-04
YNL141W	6.69E-04
YOL136C	1.32E-04

Table S2. (Continued).

YGR030C	3.05E-04
YOR074C	2.38E-04
YLR363W-A	1.86E-04
YPL157W	3.39E-04
YLR407W	2.46E-04
YBR105C	1.90E-04
YOL126C	4.45E-04
YGL209W	6.07E-04
YHL028W	1.86E-04
YJR055W	3.77E-06
YDR297W	7.47E-06
YBR157C	6.51E-05
YBR085W	1.54E-04
YOR302W	4.10E-05
YBR072W	2.89E-04
YJL218W	2.16E-04
YDR044W	1.71E-05
YDR277C	4.32E-04
YBR054W	5.61E-04
YGR035C	5.64E-04
YPL095C	1.87E-05
YHR092C	1.61E-04
YER011W	1.91E-04
YBL029W	3.86E-05
YDL039C	7.92E-04
YAR035C-A	8.23E-04
YOR338W	8.32E-05
YMR319C	6.76E-05
YKR075C	1.26E-04
YJR047C	2.10E-04
YIR042C	3.23E-05
YOR032C	3.22E-04
YDL038C	1.10E-04

Table S3. Interaction-significant genes whose expression levels were significantly changed (P < 0.001) in response to the interactive effect of plasmid bearing and oxygen limitation.

ID	Adj. P-value
YAL009W	5.59E-05
YBL029W	6.66E-04
YBL033C	2.95E-04
YBR054W	6.69E-04
YBR067C	9.10E-04
YBR071W	7.01E-07
YBR269C	2.17E-04
YCL049C	1.10E-04
YDL038C	9.41E-04
YDL227C	3.76E-04
YDR075W	1.45E-04
YDR079W	9.72E-04
YDR141C	8.27E-04
YDR189W	2.70E-04
YDR277C	2.53E-04
YDR299W	7.14E-04
YDR345C	2.10E-05
YDR434W	2.51E-04
YEL017W	6.37E-05
YEL039C	3.87E-04
YEL051W	3.65E-04
YER053C-A	1.96E-04
YER143W	3.50E-04
YGL055W	2.86E-04
YGL158W	9.43E-04
YGR043C	7.02E-04
YGR138C	2.19E-04
YGR140W	1.98E-04
YGR215W	2.57E-05
YGR217W	7.72E-04
YHL028W	7.78E-05
YHR098C	4.10E-04
YHR181W	5.88E-04
YIL069C	9.75E-05
YIL114C	6.13E-04
YIL119C	8.43E-04
YJL183W	5.44E-05
YJL196C	6.47E-04
YJL217W	3.05E-04
YJR024C	2.34E-04
YKL007W	9.79E-04
YKL040C	6.38E-04
YKL074C	5.96E-04
YKL085W	2.03E-04
YKL159C	2.05E-04
YKL165C	4.68E-05
YKR075C	2.12E-04
YLR118C	9.28E-05
YLR129W	9.52E-06
YLR224W	7.31E-04
YML027W	4.75E-04
YML030W	9.85E-04
YMR011W	2.01E-05
YMR026C	5.96E-05
YMR087W	2.34E-04
YMR271C	7.79E-04
YNL036W	2.91E-05
YNL040W	8.72E-04
YNL058C	5.99E-04
YNL100W	9.22E-05
YNL118C	6.16E-04
YNL234W	8.68E-04
YNL289W	9.42E-04
YOL123W	7.40E-04
YOL136C	4.61E-04
YOR131C	8.21E-04
YOR187W	5.67E-04
YOR236W	6.19E-04
YOR312C	1.10E-04
YPL052W	3.06E-04
YPL085W	3.90E-04
YPR002W	6.54E-04

Table S3. (Continued).

Table S4. Enriched GO biological process terms (P < 0.01) of the upregulated strain-significant genes.

Gene Ontology term	Corrected P-value
Fungal-type cell wall organization or biogenesis	3.04E-10
Cell wall organization or biogenesis	8.07E-09
Single-organism process	9.13E-09
External encapsulating structure organization	1.61E-06
Cell wall organization	1.61E-06
Fungal-type cell wall organization	4.09E-06
Single-organism catabolic process	5.72E-06
Response to extracellular stimulus	3.47E-05
Catabolic process	4.56E-05
Response to external stimulus	7.98E-05
Fungal-type cell wall biogenesis	0.00014
Cellular response to extracellular stimulus	0.00016
Cellular response to external stimulus	0.00016
Cellular catabolic process	0.00033
Response to chemical	0.00053
Cell wall biogenesis	0.00087
Response to stress	0.00107
Response to endoplasmic reticulum stress	0.00135
ER-associated ubiquitin-dependent protein catabolic process	0.00206
ERAD pathway	0.00206
Carbohydrate metabolic process	0.00246
Single-organism cellular process	0.00249
Organelle disassembly	0.00275
Response to nutrient levels	0.00366
Single-organism metabolic process	0.00628
Cellular response to stress	0.0077
Actin cytoskeleton organization	0.00794
Organic substance catabolic process	0.00958

Table S5. Enriched GO biological process terms (P < 0.01) of the downregulated strain-significant genes.

Gene Ontology term	Corrected P-value
Ribosome biogenesis	1.23E-24
Ribonucleoprotein complex biogenesis	1.97E-21
rRNA metabolic process	3.10E-19
rRNA processing	4.62E-19
ncRNA processing	7.43E-18
ncRNA metabolic process	6.90E-17
RNA processing	3.43E-13
Cellular process	2.67E-12
Ribosomal small subunit biogenesis	6.36E-11
Maturation of SSU-rRNA from tricistronic rRNA transcript (SSU-rRNA, 5.8S rRNA, LSU-rRNA)	3.35E-10
Maturation of 5.8S rRNA	4.56E-10
Maturation of 5.8S rRNA from tricistronic rRNA transcript (SSU-rRNA, 5.8S rRNA, LSU-rRNA)	4.56E-10
Cellular component biogenesis	2.27E-09
Maturation of SSU-rRNA	3.22E-09
Organic cyclic compound metabolic process	1.73E-08
Nitrogen compound metabolic process	3.74E-08
Heterocycle metabolic process	4.72E-08
Cellular aromatic compound metabolic process	8.78E-08
Ribosomal large subunit biogenesis	1.06E-07
Nucleobase-containing compound metabolic process	1.62E-07
Single-organism biosynthetic process	1.27E-06
Cleavage involved in rRNA processing	3.04E-06
Cellular nitrogen compound metabolic process	4.65E-05
RNA metabolic process	6.24E-05
Cellular component organization or biogenesis	8.97E-05
Nucleic acid metabolic process	0.00015
Cellular metabolic process	0.00036
Transmembrane transport	0.00054
Primary metabolic process	0.00057
Maturation of LSU-rRNA from tricistronic rRNA transcript (SSU-rRNA, 5.8S rRNA, LSU-rRNA)	0.00068
Endonucleolytic cleavage in ITS1 to separate SSU-rRNA from 5.8S rRNA and LSU-rRNA from tricistronic rRNA transcript (SSU-rRNA, 5.8S rRNA, LSU-rRNA)	0.00097
Organic substance metabolic process	0.00116
Endonucleolytic cleavage to generate mature 5'-end of SSU-rRNA from (SSU-rRNA, 5.8S rRNA, LSU-rRNA)	0.00217
Metabolic process	0.00217
Nucleic acid phosphodiester bond hydrolysis	0.00267
RNA phosphodiester bond hydrolysis	0.00278
rRNA 5'-end processing	0.00298
ncRNA 5'-end processing	0.00298
Maturation of LSU-rRNA	0.00394
Single-organism cellular process	0.00398
RNA 5'-end processing	0.00403
Endonucleolytic cleavage involved in rRNA processing	0.00446
Endonucleolytic cleavage of tricistronic rRNA transcript (SSU-rRNA, 5.8S rRNA, LSU-rRNA)	0.00446
Nuclear polyadenylation-dependent mRNA catabolic process	0.00868
Polyadenylation-dependent mRNA catabolic process	0.00868
Endonucleolytic cleavage in 5'-ETS of tricistronic rRNA transcript (SSU-rRNA, 5.8S rRNA, LSU-rRNA)	0.00942

Table S6. Enriched GO biological process terms (P < 0.01) of the upregulated aeration-significant genes.

Gene Ontology term	Corrected P-value
Single-organism process	3.58E-07
Single-organism cellular process	4.77E-07
Cellular response to stimulus	2.81E-05
Response to stimulus	3.36E-05
Catabolic process	0.00028
Biological regulation	0.0003
Cellular catabolic process	0.00142
Organic substance catabolic process	0.00164
Regulation of biological quality	0.00181
Cellular response to stress	0.00309
Cellular process	0.00705
Single-organism localization	0.00718
Cellular macromolecule catabolic process	0.00885

Table S7. Enriched GO biological process terms (P < 0.01) of the downregulated aeration-significant genes.

Gene Ontology term	Corrected P-value
Small molecule metabolic process	7.74E-05
Single-organism biosynthetic process	0.00013
Organic cyclic compound metabolic process	0.00091
Heterocycle metabolic process	0.00574
Cellular aromatic compound metabolic process	0.00706
Lipid biosynthetic process	0.00989

Table S8. GO biological processes that the interactive significant genes annotated to in aerated conditions were compared to microaerated conditions.

Interaction effect	Reference strain	
	GO term GO ID	Genes annotated to the GO term
UP aerated vs. microaerated	Mitochondrion organization GO:0007005	FMP21, PET100, RSM27, YML030W, YNL100W
	Lipid metabolic process GO:0006629	ELO1, GPI17, MCD4, PDH1, YLR118C
	Protein complex biogenesis GO:0070271	FMP21, PET100, SEC16, SFB3, YML030W
	Cell wall organization or biogenesis GO:0071554	MCD4, RPI1, WSC4
	Monocarboxylic acid metabolic process GO:0032787	ELO1, PDH1, YLR118C
	Nucleobase-containing small molecule metabolic process GO:0055086	CYC7, YGR043C, YJR024C
	Golgi vesicle transport GO:0048193	SEC16, SFB3
	Cellular amino acid metabolic process GO:0006520	YJR024C, YNL040W
	Generation of precursor metabolites and energy GO:0006091	CYC7, MDH1
	Response to oxidative stress GO:0006979	NCE103, YGR043C
	Vesicle organization GO:0016050	SEC16, SFB3
	Carbohydrate metabolic process GO:0005975	MDH1, YGR043C
	Cellular respiration GO:0045333	CYC7, MDH1
	Cofactor metabolic process GO:0051186	YGR043C, YJR024C
	Response to chemical GO:0042221	NCE103, YGR043C
	Ion transport GO:0006811	CCH1, MCD4
	Transcription from RNA polymerase II promoter GO:0006366	RPI1, YOX1
	Protein lipidation GO:0006497	GPI17, MCD4
	Regulation of protein modification process GO:0031399	PCL1
	Protein targeting GO:0006605	WSC4
	Cytoplasmic translation GO:0002181	RPL20B
	Protein phosphorylation GO:0006468	PCL1
	Response to heat GO:0009408	WSC4
	Nucleobase-containing compound transport GO:0015931	MCD4
	tRNA aminoacylation for protein translation GO:0006418	YNL040W
	Cytoskeleton organization GO:0007010	PCL1
	RNA splicing GO:0008380	YMR087W
	Regulation of cell cycle GO:0051726	PCL1
	DNA recombination GO:0006310	HO
	Mitotic cell cycle GO:0000278	YOX1
	Regulation of transport GO:0051049	CCH1
	Mitochondrial translation GO:0032543	RSM27
	Signaling GO:0023052	RPI1
	RNA catabolic process GO:0006401	HRP1
	mRNA processing GO:0006397	HRP1
	Transmembrane transport GO:0055085	CCH1
	tRNA processing GO:0008033	YMR087W
	Response to starvation GO:0042594	PCL1
	Protein maturation GO:0051604	HO

Table S8. (Continued).

DOWN Aerated vs. microaerated	Transmembrane transport GO:0055085	HXT2, HXT3, PEX12, POR2, TPO2, VMA8
	Regulation of organelle organization GO:0033043	CAP1, PPH3, RCK1, SLY1
	Protein complex biogenesis GO:0070271	CAP1, CBF2, DCP2, SLY1
	Proteolysis involved in cellular protein catabolic process GO:0051603	DDI1, OAZ1, YLR224W
	Golgi vesicle transport GO:0048193	DOP1, SLY1, SVP26
	rRNA processing GO:0006364	BFR2, DIP2, RPS24B
	Carbohydrate transport GO:0008643	HXT2, HXT3, MTH1
	Nucleobase-containing small molecule metabolic process GO:0055086	DFR1, PFK27, URA10
	Ribosomal small subunit biogenesis GO:0042274	BFR2, DIP2, RPS24B
	Carbohydrate metabolic process GO:0005975	MNN11, PFK27, SVP26
	Signaling GO:0023052	MTH1, PPH3, RCN1
	Ion transport GO:0006811	POR2, TPO2, VMA8
	Organelle fission GO:0048285	PPH3, RCK1
	Organelle assembly GO:0070925	CBF2, DCP2
	Monocarboxylic acid metabolic process GO:0032787	OLE1, PFK27
	Cytoskeleton organization GO:0007010	CAP1, CBF2
	Regulation of cell cycle GO:0051726	PPH3, RCK1
	Lipid metabolic process GO:0006629	OLE1, SPO7
	Protein glycosylation GO:0006486	MNN11, SVP26
	Translational elongation GO:0006414	OAZ1, RPS24B
	Regulation of transport GO:0051049	POR2, SLY1
	Meiotic cell cycle GO:0051321	PPH3, RCK1
	Protein modification by small protein conjugation or removal GO:0070647	PEX12, YLR224W
	Protein dephosphorylation GO:0006470	PPH3, SPO7
	Cofactor metabolic process GO:0051186	DFR1, PFK27
	mRNA processing GO:0006397	DCP2, MUD2
	Response to chemical GO:0042221	PPH3, YLR224W
	Cellular ion homeostasis GO:0006873	NFU1, VMA8
	Nucleus organization GO:0006997	SPO7
	Regulation of protein modification process GO:0031399	SPO7
	DNA-templated transcription, initiation GO:0006352	DCP2
	Cell wall organization or biogenesis GO:0071554	SVP26
	Peroxisome organization GO:0007031	PEX12
	Protein targeting GO:0006605	PEX12
	Vitamin metabolic process GO:0006766	RIB1
	Cellular amino acid metabolic process GO:0006520	DFR1
	Cytoplasmic translation GO:0002181	RPS24B
	Protein phosphorylation GO:0006468	RCK1
	Generation of precursor metabolites and energy GO:0006091	PFK27
	Nucleobase-containing compound transport GO:0015931	POR2
	Organelle inheritance GO:0048308	OLE1
	Mitochondrion organization GO:0007005	OLE1
	RNA splicing GO:0008380	MUD2
	DNA recombination GO:0006310	PPH3
	Mitotic cell cycle GO:0000278	CBF2
	Chromosome segregation GO:0007059	CBF2
	Vesicle organization GO:0016050	SLY1
	Membrane fusion GO:0061025	SLY1
	Organelle fusion GO:0048284	SLY1
	Cellular response to DNA damage stimulus GO:0006974	PPH3
	RNA catabolic process GO:0006401	DCP2
	Cell morphogenesis GO:0000902	DOP1
	Endosomal transport GO:0016197	DOP1
	DNA repair GO:0006281	PPH3
	Sporulation GO:0043934	SPO7
	Regulation of DNA metabolic process GO:0051052	PPH3
	Regulation of translation GO:0006417	OAZ1
	Transcription from RNA polymerase II promoter GO:0006366	DCP2
	Conjugation GO:0000746	YDL038C
	Exocytosis GO:0006887	SLY1

Table S8. (Continued).

Interaction effect	WTPB-G	
	GO term GO ID	Genes annotated to the GO term
UP aerated vs. microaerated	Protein complex biogenesis GO:0070271	CBF2, DCP2, SEC16, SFB3, SLY1
	Golgi vesicle transport GO:0048193	DOP1, SEC16, SFB3, SLY1
	Lipid metabolic process GO:0006629	GPI17, MCD4, OLE1, PDH1
	Proteolysis involved in cellular protein catabolic process GO:0051603	DDI1, OAZ1, YLR224W
	Vesicle organization GO:0016050	SEC16, SFB3, SLY1
	Transmembrane transport GO:0055085	CCH1, HXT2, PEX12
	Response to chemical GO:0042221	NCE103, YGR043C, YLR224W
	Cellular amino acid metabolic process GO:0006520	DFR1, YNL040W
	Organelle assembly GO:0070925	CBF2, DCP2
	Response to oxidative stress GO:0006979	NCE103, YGR043C
	Carbohydrate transport GO:0008643	HXT2, MTH1
	Monocarboxylic acid metabolic process GO:0032787	OLE1, PDH1
	Nucleobase-containing small molecule metabolic process GO:0055086	DFR1, YGR043C
	Regulation of transport GO:0051049	CCH1, SLY1
	Regulation of organelle organization GO:0033043	RCK1, SLY1
	Protein modification by small protein conjugation or removal GO:0070647	PEX12, YLR224W
	Cofactor metabolic process GO:0051186	DFR1, YGR043C
	mRNA processing GO:0006397	DCP2, MUD2
	Ion transport GO:0006811	CCH1, MCD4
	Protein lipidation GO:0006497	GPI17, MCD4
	DNA-templated transcription, initiation GO:0006352	DCP2
	Organelle fission GO:0048285	RCK1
	Cell wall organization or biogenesis GO:0071554	MCD4
	Peroxisome organization GO:0007031	PEX12
	Protein targeting GO:0006605	PEX12
	Vitamin metabolic process GO:0006766	RIB1
	Protein phosphorylation GO:0006468	RCK1
	Nucleobase-containing compound transport GO:0015931	MCD4
	Organelle inheritance GO:0048308	OLE1
	Mitochondrion organization GO:0007005	OLE1
	tRNA aminoacylation for protein translation GO:0006418	YNL040W
	Cytoskeleton organization GO:0007010	CBF2
	RNA splicing GO:0008380	MUD2
	Regulation of cell cycle GO:0051726	RCK1
	Mitotic cell cycle GO:0000278	CBF2
	Chromosome segregation GO:0007059	CBF2
	Translational elongation GO:0006414	OAZ1
	Membrane fusion GO:0061025	SLY1
	Organelle fusion GO:0048284	SLY1
	Meiotic cell cycle GO:0051321	RCK1
	Carbohydrate metabolic process GO:0005975	YGR043C
	Signaling GO:0023052	MTH1
	RNA catabolic process GO:0006401	DCP2
	Cell morphogenesis GO:0000902	DOP1
	Endosomal transport GO:0016197	DOP1
	Regulation of translation GO:0006417	OAZ1
	Transcription from RNA polymerase II promoter GO:0006366	DCP2
	Exocytosis GO:0006887	SLY1

Table S8. (Continued).

DOWN Aerated vs. microaerated	Mitochondrion organization GO:0007005	FMP21, PET100, RSM27, YML030W, YNL100W
	Nucleobase-containing small molecule metabolic process GO:0055086	CYC7, PFK27, URA10, YJR024C
	Carbohydrate metabolic process GO:0005975	MDH1, MNN11, PFK27, SVP26
	Transmembrane transport GO:0055085	HXT3, POR2, TPO2, VMA8
	Protein complex biogenesis GO:0070271	CAP1, FMP21, PET100, YML030W
	Cell wall organization or biogenesis GO:0071554	RPI1, SVP26, WSC4
	Generation of precursor metabolites and energy GO:0006091	CYC7, MDH1, PFK27
	rRNA processing GO:0006364	BFR2, DIP2, RPS24B
	Monocarboxylic acid metabolic process GO:0032787	ELO1, PFK27, YLR118C
	Lipid metabolic process GO:0006629	ELO1, SPO7, YLR118C
	Ribosomal small subunit biogenesis GO:0042274	BFR2, DIP2, RPS24B
	Signaling GO:0023052	PPH3, RCN1, RPI1
	Ion transport GO:0006811	POR2, TPO2, VMA8
	Regulation of protein modification process GO:0031399	PCL1, SPO7
	Cytoplasmic translation GO:0002181	RPL20B, RPS24B
	Cytoskeleton organization GO:0007010	CAP1, PCL1
	Regulation of cell cycle GO:0051726	PCL1, PPH3
	DNA recombination GO:0006310	HO, PPH3
	Protein glycosylation GO:0006486	MNN11, SVP26
	Regulation of organelle organization GO:0033043	CAP1, PPH3
	Protein dephosphorylation GO:0006470	PPH3, SPO7
	Cellular respiration GO:0045333	CYC7, MDH1
	Cofactor metabolic process GO:0051186	PFK27, YJR024C
	Cellular ion homeostasis GO:0006873	NFU1, VMA8
	Transcription from RNA polymerase II promoter GO:0006366	RPI1, YOX1
	Nucleus organization GO:0006997	SPO7
	Organelle fission GO:0048285	PPH3
	Golgi vesicle transport GO:0048193	SVP26
	Protein targeting GO:0006605	WSC4
	Cellular amino acid metabolic process GO:0006520	YJR024C
	Protein phosphorylation GO:0006468	PCL1
	Response to heat GO:0009408	WSC4
	Nucleobase-containing compound transport GO:0015931	POR2
	Carbohydrate transport GO:0008643	HXT3
	RNA splicing GO:0008380	YMR087W
	Mitotic cell cycle GO:0000278	YOX1
	translational elongation GO:0006414	RPS24B
	Regulation of transport GO:0051049	POR2
	Meiotic cell cycle GO:0051321	PPH3
	Mitochondrial translation GO:0032543	RSM27
	Cellular response to DNA damage stimulus GO:0006974	PPH3
	RNA catabolic process GO:0006401	HRP1
	mRNA processing GO:0006397	HRP1
	DNA repair GO:0006281	PPH3
	Response to chemical GO:0042221	PPH3
	Sporulation GO:0043934	SPO7
	Regulation of DNA metabolic process GO:0051052	PPH3
	tRNA processing GO:0008033	YMR087W
	Response to starvation GO:0042594	PCL1
	Protein maturation GO:0051604	HO
	Conjugation GO:0000746	YDL038C

Table S9. GO biological processes that the interactive significant genes annotated to in the reference strain were compared to the WTPB-G strain.

Interaction effect	Aerated conditions	
	GO term GO ID	Genes annotated to the GO term
UP (WTPB-G vs. reference strain)	Protein complex biogenesis GO:0070271	CAP1, DCP2, FMP21, SEC16, SFB3, SLY1
	Golgi vesicle transport GO:0048193	DOP1, SEC16, SFB3, SLY1
	Nucleobase-containing small molecule metabolic process GO:0055086	DFR1, URA10, YGR043C, YJR024C
	Proteolysis involved in cellular protein catabolic process GO:0051603	DDI1, OAZ1, YLR224W
	Cellular amino acid metabolic process GO:0006520	DFR1, YJR024C, YNL040W
	Lipid metabolic process GO:0006629	GPI17, MCD4, OLE1
	Vesicle organization GO:0016050	SEC16, SFB3, SLY1
	Regulation of organelle organization GO:0033043	CAP1, RCK1, SLY1
	Cofactor metabolic process GO:0051186	DFR1, YGR043C, YJR024C
	Transmembrane transport GO:0055085	CCH1, HXT2, PEX12
	Response to chemical GO:0042221	NCE103, YGR043C, YLR224W
	Protein phosphorylation GO:0006468	PCL1, RCK1
	Mitochondrion organization GO:0007005	FMP21, OLE1
	Response to oxidative stress GO:0006979	NCE103, YGR043C
	Cytoskeleton organization GO:0007010	CAP1, PCL1
	RNA splicing GO:0008380	MUD2, YMR087W
	Regulation of cell cycle GO:0051726	PCL1, RCK1
	Regulation of transport GO:0051049	CCH1, SLY1
	Protein modification by small protein conjugation or removal GO:0070647	PEX12, YLR224W
	mRNA processing GO:0006397	DCP2, MUD2
	Ion transport GO:0006811	CCH1, MCD4
	Protein lipidation GO:0006497	GPI17, MCD4
	Regulation of protein modification process GO:0031399	PCL1
	DNA-templated transcription, initiation GO:0006352	DCP2
	Organelle fission GO:0048285	RCK1
	Cell wall organization or biogenesis GO:0071554	MCD4
	Protein targeting GO:0006605	PEX12
	Peroxisome organization GO:0007031	PEX12
	Vitamin metabolic process GO:0006766	RIB1
	Organelle assembly GO:0070925	DCP2
	Nucleobase-containing compound transport GO:0015931	MCD4
	Organelle inheritance GO:0048308	OLE1
	Monocarboxylic acid metabolic process GO:0032787	OLE1
	Carbohydrate transport GO:0008643	HXT2
	tRNA aminoacylation for protein translation GO:0006418	YNL040W
	Translational elongation GO:0006414	OAZ1
	Membrane fusion GO:0061025	SLY1
	Organelle fusion GO:0048284	SLY1
	Meiotic cell cycle GO:0051321	RCK1
	Carbohydrate metabolic process GO:0005975	YGR043C
	Signaling GO:0023052	RCN1
	Endosomal transport GO:0016197	DOP1
	Cell morphogenesis GO:0000902	DOP1
	RNA catabolic process GO:0006401	DCP2
	Regulation of translation GO:0006417	OAZ1
	Transcription from RNA polymerase II promoter GO:0006366	DCP2
	tRNA processing GO:0008033	YMR087W
	Response to starvation GO:0042594	PCL1
	Conjugation GO:0000746	YDL038C
	Exocytosis GO:0006887	SLY1

Table S9. (Continued).

DOWN (WTPB-G vs. reference strain)	Mitochondrion organization GO:0007005	PET100, RSM27, YML030W, YNL100W
	Monocarboxylic acid metabolic process GO:0032787	ELO1, PDH1, PFK27, YLR118C
	Lipid metabolic process GO:0006629	ELO1, PDH1, SPO7, YLR118C
	Carbohydrate metabolic process GO:0005975	MDH1, MNN11, PFK27, SVP26
	Transmembrane transport GO:0055085	HXT3, POR2, TPO2, VMA8
	Cell wall organization or biogenesis GO:0071554	RPI1, SVP26, WSC4
	Generation of precursor metabolites and energy GO:0006091	CYC7, MDH1, PFK27
	rRNA processing GO:0006364	BFR2, DIP2, RPS24B
	Ribosomal small subunit biogenesis GO:0042274	BFR2, DIP2, RPS24B
	Signaling GO:0023052	MTH1, PPH3, RPI1
	Ion transport GO:0006811	POR2, TPO2, VMA8
	Protein complex biogenesis GO:0070271	CBF2, PET100, YML030W
	Cytoplasmic translation GO:0002181	RPL20B, RPS24B
	Carbohydrate transport GO:0008643	HXT3, MTH1
	Nucleobase-containing small molecule metabolic process GO:0055086	CYC7, PFK27
	DNA recombination GO:0006310	HO, PPH3
	Mitotic cell cycle GO:0000278	CBF2, YOX1
	Protein glycosylation GO:0006486	MNN11, SVP26
	Protein dephosphorylation GO:0006470	PPH3, SPO7
	Cellular respiration GO:0045333	CYC7, MDH1
	Cellular ion homeostasis GO:0006873	NFU1, VMA8
	Transcription from RNA polymerase II promoter GO:0006366	RPI1, YOX1
	Nucleus organization GO:0006997	SPO7
	Regulation of protein modification process GO:0031399	SPO7
	Organelle fission GO:0048285	PPH3
	Golgi vesicle transport GO:0048193	SVP26
	Protein targeting GO:0006605	WSC4
	Organelle assembly GO:0070925	CBF2
	Response to heat GO:0009408	WSC4
	Nucleobase-containing compound transport GO:0015931	POR2
	Cytoskeleton organization GO:0007010	CBF2
	Regulation of cell cycle GO:0051726	PPH3
	Chromosome segregation GO:0007059	CBF2
	Translational elongation GO:0006414	RPS24B
	Regulation of transport GO:0051049	POR2
	Regulation of organelle organization GO:0033043	PPH3
	Meiotic cell cycle GO:0051321	PPH3
	Mitochondrial translation GO:0032543	RSM27
	Cellular response to DNA damage stimulus GO:0006974	PPH3
	Cofactor metabolic process GO:0051186	PFK27
	RNA catabolic process GO:0006401	HRP1
	mRNA processing GO:0006397	HRP1
	DNA repair GO:0006281	PPH3
	Response to chemical GO:0042221	PPH3
	Sporulation GO:0043934	SPO7
	Regulation of DNA metabolic process GO:0051052	PPH3
	Protein maturation GO:0051604	HO

Table S9. (Continued).

Interaction effect	Microaerated conditions	
	GO term GO ID	Genes annotated to the GO term
UP (WTPB-G vs. reference strain)	Protein complex biogenesis GO:0070271	CAP1, FMP21, SEC16, SFB3, SLY1, YML030W
	Lipid metabolic process GO:0006629	GPI17, MCD4, OLE1, SPO7, YLR118C
	Ion transport GO:0006811	CCH1, MCD4, POR2, TPO2, VMA8
	Golgi vesicle transport GO:0048193	DOP1, SEC16, SFB3, SLY1
	Mitochondrion organization GO:0007005	FMP21, OLE1, YML030W, YNL100W
	Nucleobase-containing small molecule metabolic process GO:0055086	DFR1, URA10, YGR043C, YJR024C
	Transmembrane transport GO:0055085	CCH1, POR2, TPO2, VMA8
	Cell wall organization or biogenesis GO:0071554	MCD4, RPI1, WSC4
	Cellular amino acid metabolic process GO:0006520	DFR1, YJR024C, YNL040W
	Regulation of transport GO:0051049	CCH1, POR2, SLY1
	Vesicle organization GO:0016050	SEC16, SFB3, SLY1
	Cofactor metabolic process GO:0051186	DFR1, YGR043C, YJR024C
	Regulation of protein modification process GO:0031399	PCL1, SPO7
	Nucleobase-containing compound transport GO:0015931	MCD4, POR2
	Monocarboxylic acid metabolic process GO:0032787	OLE1, YLR118C
	Cytoskeleton organization GO:0007010	CAP1, PCL1
	RNA splicing GO:0008380	MUD2, YMR087W
	Regulation of organelle organization GO:0033043	CAP1, SLY1
	Signaling GO:0023052	RCN1, RPI1
	Cellular ion homeostasis GO:0006873	NFU1, VMA8
	Transcription from RNA polymerase II promoter GO:0006366	RPI1, YOX1
	Protein lipidation GO:0006497	GPI17, MCD4
	Nucleus organization GO:0006997	SPO7
	Proteolysis involved in cellular protein catabolic process GO:0051603	OAZ1
	Protein targeting GO:0006605	WSC4
	Protein phosphorylation GO:0006468	PCL1
	Organelle inheritance GO:0048308	OLE1
	Response to heat GO:0009408	WSC4
	Response to oxidative stress GO:0006979	YGR043C
	RNA aminoacylation for protein translation GO:0006418	YNL040W
	Regulation of cell cycle GO:0051726	PCL1
	Mitotic cell cycle GO:0000278	YOX1
	Translational elongation GO:0006414	OAZ1
	Membrane fusion GO:0061025	SLY1
	Organelle fusion GO:0048284	SLY1
	Carbohydrate metabolic process GO:0005975	YGR043C
	Protein dephosphorylation GO:0006470	SPO7
	mRNA processing GO:0006397	MUD2
	Endosomal transport GO:0016197	DOP1
	Cell morphogenesis GO:0000902	DOP1
	Response to chemical GO:0042221	YGR043C
	Sporulation GO:0043934	SPO7
	Regulation of translation GO:0006417	OAZ1
	tRNA processing GO:0008033	YMR087W
	Response to starvation GO:0042594	PCL1
	Exocytosis GO:0006887	SLY1

Table S9. (Continued).

DOWN (WTPB-G vs. reference strain)	Carbohydrate metabolic process GO:0005975	MDH1, MNN11, PFK27, SVP26
	Generation of precursor metabolites and energy GO:0006091	CYC7, MDH1, PFK27
	rRNA processing GO:0006364	BFR2, DIP2, RPS24B
	Monocarboxylic acid metabolic process GO:0032787	ELO1, PDH1, PFK27
	Carbohydrate transport GO:0008643	HXT2, HXT3, MTH1
	Ribosomal small subunit biogenesis GO:0042274	BFR2, DIP2, RPS24B
	Transmembrane transport GO:0055085	HXT2, HXT3, PEX12
	Response to chemical GO:0042221	NCE103, PPH3, YLR224W
	Protein complex biogenesis GO:0070271	CBF2, DCP2, PET100
	Proteolysis involved in cellular protein catabolic process GO:0051603	DDI1, YLR224W
	Organelle fission GO:0048285	PPH3, RCK1
	Cytoplasmic translation GO:0002181	RPL20B, RPS24B
	Organelle assembly GO:0070925	CBF2, DCP2
	Mitochondrion organization GO:0007005	PET100, RSM27
	Nucleobase-containing small molecule metabolic process GO:0055086	CYC7, PFK27
	Regulation of cell cycle GO:0051726	PPH3, RCK1
	DNA recombination GO:0006310	HO, PPH3
	Lipid metabolic process GO:0006629	ELO1, PDH1
	Protein glycosylation GO:0006486	MNN11, SVP26
	Regulation of organelle organization GO:0033043	PPH3, RCK1
	protein modification by small protein conjugation or removal GO:0070647	PEX12, YLR224W
	Meiotic cell cycle GO:0051321	PPH3, RCK1
	Signaling GO:0023052	MTH1, PPH3
	Cellular respiration GO:0045333	CYC7, MDH1
	RNA catabolic process GO:0006401	DCP2, HRP1
	mRNA processing GO:0006397	DCP2, HRP1
	DNA-templated transcription, initiation GO:0006352	DCP2
	Golgi vesicle transport GO:0048193	SVP26
	Peroxisome organization GO:0007031	PEX12
	Protein targeting GO:0006605	PEX12
	Cell wall organization or biogenesis GO:0071554	SVP26
	Vitamin metabolic process GO:0006766	RIB1
	Protein phosphorylation GO:0006468	RCK1
	Response to oxidative stress GO:0006979	NCE103
	Cytoskeleton organization GO:0007010	CBF2
	Mitotic cell cycle GO:0000278	CBF2
	Chromosome segregation GO:0007059	CBF2
	Translational elongation GO:0006414	RPS24B
	Mitochondrial translation GO:0032543	RSM27
	Protein dephosphorylation GO:0006470	PPH3
	Cellular response to DNA damage stimulus GO:0006974	PPH3
	Cofactor metabolic process GO:0051186	PFK27
	DNA repair GO:0006281	PPH3
	Regulation of DNA metabolic process GO:0051052	PPH3
	Transcription from RNA polymerase II promoter GO:0006366	DCP2
	Protein maturation GO:0051604	HO
	Conjugation GO:0000746	YDL038C